THE JOURNAL OF GENE MEDICINE
J Gene Med 2006; 8: 824–834.
Published online 20 April 2006 in Wiley InterScience (www.interscience.wiley.com) **DOI:** 10.1002/jgm.910

RESEARCH ARTICLE

Enhanced DNA vaccine potency by mannosylated lipoplex after intraperitoneal administration

Yoshiyuki Hattori
Shigeru Kawakami
Yan Lu
Kazumi Nakamura
Fumiyoshi Yamashita
Mitsuru Hashida*

Department of Drug Delivery Research, Graduate School of Pharmaceutical Sciences, Kyoto University, Sakyo-ku, Kyoto 606-8501, Japan

*Correspondence to:
Mitsuru Hashida, Department of Drug Delivery Research, Graduate School of Pharmaceutical Sciences, Kyoto University, Sakyo-ku, Kyoto 606-8501, Japan. E-mail: hashidam@pharm.kyoto-u.ac.jp

Abstract

Background Here we describe a novel DNA vaccine formulation that can enhance cytotoxic T lymphocyte (CTL) activity through efficient gene delivery to dendritic cells (DCs) by mannose receptor-mediated endocytosis.

Methods Ovalbumin (OVA) was selected as a model antigen for vaccination; accordingly, OVA-encoding pDNA (pCMV-OVA) was constructed to evaluate DNA vaccination. Mannosylated cationic liposomes (Man-liposomes) were prepared using cholesten-5-yloxy-*N*-{4-[(1-imino-2-D-thiomannosylethyl)amino]butyl}formamide (Man-C4-Chol) with cationic lipid. The potency of the mannosylated liposome/pCMV-OVA complex (Man-lipoplex) was evaluated by measuring OVA mRNA in $CD11c^+$ cells, CTL activity, and the OVA-specific anti-tumor effect after *in vivo* administration.

Results An *in vitro* study using DC2.4 cells demonstrated that Man-liposomes could transfect pCMV-OVA more efficiently than cationic liposomes via mannose receptor-mediated endocytosis. *In vivo* studies revealed that the Man-lipoplex exhibited higher OVA mRNA expression in $CD11c^+$ cells in the spleen and peritoneal cavity and provided a stronger OVA-specific CTL response than intraperitoneal (i.p.) administration of the conventional lipoplex and intramuscular (i.m.) administration of naked pCMV-OVA, the standard protocol for DNA vaccination. Pre-immunization with the Man-lipoplex provided much better OVA-specific anti-tumor effect than naked pCMV-OVA via the i.m. route.

Conclusions These results suggested that *in vivo* active targeting of DNA vaccine to DCs with Man-lipoplex might prove useful for the rational design of DNA vaccine. Copyright © 2006 John Wiley & Sons, Ltd.

Keywords gene therapy; DNA vaccine; mannosylated liposomes; non-viral vectors

Introduction

DNA vaccine, plasmid DNA (pDNA)-encoding antigen from a pathogen, is of great interest in gene therapy as a means of immunotherapy against refractory diseases such as cancer and viral infections because the administration of naked pDNA-encoding antigen proteins induces not only an antibody response, but also a potent cytotoxic T lymphocyte (CTL) response in animal models [1–3]. Recent immunological studies have demonstrated that gene transfection and subsequent activation of antigen-presenting cells (APCs), dendritic cells (DCs) and macrophages are important for efficient DNA

Received: 15 December 2005
Revised: 31 January 2006
Accepted: 1 February 2006

vaccine therapy [4–6]. Although some clinical trials involving melanoma, human imuunodeficiency virus, and HCV have been performed using topical administration of naked pDNA [7–9], the results are not good enough for clinical therapy. In order to overcome this problem, it is important to develop gene delivery carriers for *in vivo* APC-selective gene transfection.

In spite of the high transfection efficiency of viral vectors, they still need to be improved from the point of view of safety issues [10–12]. The use of non-viral vectors is one of the possible approaches for *in vivo* gene delivery because they are free from some of the risks inherent in these systems. Furthermore, the characteristics of non-viral vectors can be more easily modified than those of viral vectors. To achieve targeted gene delivery, a number of receptor-mediated gene delivery systems have been developed [13–16] including our carriers [17–22]. As far as *in vivo* selective gene delivery to APCs is concerned, mannose has been shown to be a promising ligand to target APCs because these cells have a large number of mannose receptors.

Recently, we have developed several types of macromolecular [18] and particulate [22,23] gene carriers for macrophage-selective gene transfection *in vivo*. Among them, cationic liposomes containing cholesten-5-yloxy-*N*-{4-[(1-imino-2-D-thiomannosylethyl)amino]butyl} formamide (Man-C4-Chol) are some of the most interesting potential gene transfection carriers [22,23] that can be efficiently recognized by mannose receptors on macrophages in liver. Man-C4-Chol exhibits bifunctional properties, i.e., an imino group for binding to pDNA via electrostatic interaction and a mannose residue for the cell-surface receptors in APCs [22]. Therefore, a high density of mannose residues can be provided on the liposome surface without affecting the binding of the cationic liposomes to pDNA. More recently, we have demonstrated that intravenously administrated pCMV-OVA complexed with mannosylated liposomes (Man-lipoplex) enhances MHC class I antigen presentation, but no measurable CTL response was observed [24], suggesting that not only cell-selective gene transfection but also enhanced transfection efficiency in DCs is needed for gene therapy.

Intraperitoneal (i.p.) administration has some advantages as far as the transfection efficacy to DCs by Man-lipoplex is concerned; this is because of (i) high accessibility to APCs in the peritoneal cavity and lymph nodes, (ii) long retention of the lipoplex, (iii) the presence of few biocomponents that reduce transfection activity, and (iv) the high capacity of the lipoplex solution. Taking these factors into consideration, i.p. administrated Man-lipoplex would enhance gene expression in APCs resulting in efficient DNA vaccine therapy. However, few reports are available on the effect of i.p. administered Man-lipoplex on DNA vaccine therapy.

The objective of this paper was to clarify the DNA vaccine potency after i.p. administration of Man-lipoplex. In the present study, ovalbumin (OVA)-encoding pDNA (pCMV-OVA) was selected as a model DNA vaccine. Using *in vitro* and *in vivo* experiments, the transfection efficacy to APCs was evaluated by measuring the OVA mRNA using quantitative reverse-transcription polymerase chain reaction (RT-PCR). After immunizing with Man-lipoplex, OVA-specific CTL responses and its antitumor effects against inoculated E.G7-OVA cells (OVA expressing cells), and its parental cell line, EL4 cells (OVA non-expressing cells), were also evaluated. The results obtained were compared with those of conventional lipoplex and naked pCMV-OVA.

Materials and methods

Materials

Cholesteryl chloroformate, HEPES, concanavalin A, G418, and immunogloblin G were obtained from Sigma Chemicals Inc. (St. Louis, MO, USA). *N*-[1-(2,3-Dioleyloxy)propyl]-*N*,*N*,*N*-trimethylammonium chloride (DOTMA) and *N*-(4-aminobutyl)carbamic acid *tert*-butyl ester were obtained from Tokyo Chemical Industry Co. (Tokyo, Japan). Dioleoylphosphatidylethanolamine (DOPE) was purchased from Avanti Polar Lipids, Inc. (Alabaster, AL, USA). pVAX I, fetal bovine serum (FBS), and Opti-MEM I® were obtained from Invitrogen Co. (Carlsbad, CA, USA). Anti-CD11c monoclonal antibody (N418)-labeled magnetic beads were purchased from Miltenyi Biotec Inc. (Auburn, CA, USA). Nucleic acid purification kit magextractor®-RNA was purchased from Toyobo Co., Ltd. (Osaka, Japan). The first strand cDNA synthesis kit for RT-PCR, Lightcycler™ faststart DNA master hybridization probes, and a Lightcycler™-Primer/Probes set for mouse β-actin were purchased from Roche Diagnostics Co. (Indianapolis, IN, USA). Primers/probes for OVA were purchased from Nihon Gene Research Labs Inc. (Miyagi, Japan). All other chemicals were of the highest purity available.

Animals

Female ICR mice (4–5 weeks old) and C57BL/6 mice (6–8 weeks old) were purchased from the Shizuoka Agricultural Cooperative Association for Laboratory Animals (Shizuoka, Japan). All animal experiments were carried out in accordance with the Principles of Laboratory Animal Care as adopted and promulgated by the US National Institutes of Health and the guideline for animal experiments of Kyoto University.

Cell line

DC2.4 cells, a cell line of murine dendritic cells (DCs, haplotype H-2b) [25], were kindly provided by Dr. K. L. Rock (University of Massachusetts Medical School, Worcester, MA, USA). The expression of mannose receptors in this cell line has been confirmed elsewhere [26]. Therefore, DC2.4 cells are a suitable model of DCs.

EL4 cells (ATCC: TIB-39) and E.G7-OVA cells (ATCC: CRL-2113) were purchased from the American Type Culture Collection (ATCC, Manassas, VA, USA) and maintained in Dulbecco's modified Eagle's medium supplemented with 10% FBS and RPMI 1640 supplemented with 10% FBS, 4.5 g/l glucose, 10 mM HEPES, 1 mM sodium pyruvate, 0.05 mM 2-mercaptoethanol and 0.4 mg/ml G418.

Synthesis of Man-C4-Chol and Gal-C4-Chol

Man-C4-Chol and Gal-C4-Chol were synthesized as described previously [19,22]. Briefly, *N*-(4-aminobutyl)-(cholesten-5-yloxyl)formamide (C4-Chol) was synthesized from cholesteryl chloroformate and *N*-(4-aminobutyl)carbamic acid *tert*-butyl ester. The C4-Chol was reacted with 5 equivalents of 2-imino-2-methoxyethyl-1-thiomannoside or 2-imino-2-methoxyethyl-1-thiogalactoside [27] in pyridine containing 1.1 equivalents of triethylamine for 24 h. After evaporation of the reaction mixture *in vacuo*, the resultant material was suspended in water and dialyzed against water for 48 h, and then lyophilized.

Construction and preparation of pCMV-OVA

pCMV-OVA was constructed by subcloning the EcoRI chicken egg albumin (ovalbumin) cDNA fragment from pAc-neo-OVA [28], which was kindly provided by Dr. M. J. Bevan (University of Washington, Seattle, WA, USA), into the polylinker of pVAX I. pCMV-OVA was amplified in the *E. coli* strain, DH5α, then isolated, and purified using a Qiagen plasmid giga kit (Qiagen GmbH, Hilden, Germany). The endotoxin in pCMV-OVA solution was removed by the Triton X-114 method.

Preparation of cationic liposomes

Liposomes were prepared using the method reported previously [19,22]. Briefly, DOTMA, Chol, and Man-C4-Chol or Gal-C4-Chol were mixed in chloroform at a molar ratio of 2:1:1:0, 2:1:0:1, and 2:2:0:0 to prepare Man-liposomes, Gal-liposomes, and cationic liposomes, respectively. Then, the mixture was dried, vacuum desiccated, and resuspended in sterile 20 mM HEPES buffer (pH 7.8) or 5% dextrose solution in a sterile test tube for *in vitro* and *in vivo* experiments, respectively. After hydration, the dispersion was sonicated for 5 min in a bath sonicator to produce liposomes and then sterilized by passing through a 0.45 μm filter (Nihon-Millipore Ltd., Tokyo, Japan).

Preparation of lipoplex for *in vitro* study

Lipoplex was prepared using the method reported previously [19,22]. Briefly, equal volumes of pCMV-OVA and stock liposome solution were diluted with Opti-MEM I® in 15 ml Falcon tubes. Then, pCMV-OVA solution was added rapidly to the surface of the liposome solution at a charge ratio (−/+) of 1.0:2.3 using a micropipette (Pipetman®, Gilson, Villier-le Bel, France) and the mixture was agitated rapidly by pumping it up and down twice in the pipette tip.

Preparation of lipoplex for *in vivo* study

All cationic liposome/pCMV-OVA complexes for *in vivo* experiments were prepared under the optimal conditions for cell-selective gene transfection as reported previously [29–31]. Briefly, equal volumes of pCMV-OVA and stock liposome solution were diluted with 5% dextrose in 15 ml tubes. Then, pCMV-OVA solution was added rapidly to the surface of the liposome solution using a micropipette and the mixture was agitated rapidly by pumping it up and down twice in the pipette tip. The mean particle sizes were measured by dynamic light scattering spectrophotometry (LS-900; Otsuka Electronics Co., Ltd., Osaka, Japan). The zeta-potential of the lipoplexes was measured by the laser-Doppler electrophoresis method with a Zetasizer Nano ZS (Malvern Instruments Ltd., Worcestershire, UK).

Uptake characteristics by DC2.4 cells

Uptake study was performed by the method reported previously [19,22]. Briefly, the DC2.4 cells were plated on a 24-well plate at a density of 0.65×10^5 cells/cm^2 and cultivated in 500 μl RPMI supplemented with 10% FBS. Twenty-four hours later, the culture medium was replaced with an equivalent volume of Hanks medium (Nissui Pharmaceutical Co., Ltd., Tokyo, Japan) containing 1 kBq/ml [^{32}P]-pCMV-OVA, 0.5 mg/ml cold pCMV-OVA and cationic liposomes at a charge ratio (−/+) of 1.0:2.3. After incubation for given time periods, the solution was quickly removed by aspiration, the cells were washed five times with ice-cold HBSS buffer and then solubilized in 0.3 M NaOH solution with 10% Triton X-100 (0.3 ml). The radioactivity was measured by liquid scintillation counting (LSC-500; Beckman, Inc., Tokyo, Japan) and the protein content was determined by a modification of the Lowry method. The effect of the presence of 0.125 mg/ml mannan was determined in the same system.

Transfection activity by DC2.4 cells

DC2.4 cells were seeded in 10.5 cm^2 dishes at a density of 0.65×10^5 cells/cm^2 in RPMI 1640 medium supplemented with 10% FBS. After 24 h in culture, the culture medium was replaced with Opti-MEM I® containing 0.5 μg/ml pCMV-OVA and cationic liposomes. Six hours later, the incubation medium was replaced again with RPMI 1640 supplemented with 10% FBS and incubated for an additional 6 h. Then, the cells were

scraped and suspended in 200 μl pH 7.4 phosphate-buffered saline (PBS). Total RNA was isolated from DC2.4 cells with MagExtractor MFX-2000 (Toyobo Co., Ltd., Osaka, Japan) and MagExtractor-RNA following the manufacturer's instructions. Reverse transcription of mRNA was carried out using a first strand cDNA synthesis kit as follows: total RNA was added to the oligo dT primer (0.8 μg/μl) solution, and incubated at 42 °C for 60 min with a program temperature control system PC-808 (Astec Co., Ltd., Fukuoka, Japan). Real-time PCR was performed using the Lightcycler™ quick system 350S (Roche Diagnostics Co., Indianapolis, IN, USA) with hybridization probes. Primer and hybridization probes for OVA cDNA were constructed as follows: primer, 5′-GCGTCTCTGAATTTAGGG-3′ (forward) and 5′-TACCCCTGATACTACAGTGC-3′ (reverse); hybridization probes, 5′-CTTCTGTATCAAGCACATCGCAACCAACG-3′-fluorescein isothiocyanate (FITC) and Lightcycler™-Red640 (LCRed)-5′-CGTTCTCTTCTTTGGCAGATGTGT-TTCCCC-3′. The PCR reaction for detection of the OVA gene was carried out in a final volume of 20 μl containing: (i) 2 μl DNA Master hybridization probes 10× (DNA Master hybridization probes kit); (ii) 1.6 μl 25 mM $MgCl_2$; (iii) 1.5 μl forward and reverse primers (final concentration 0.75 μM); (iv) 1 μl 2 μM FITC-labeled hybridization probes and 2 μl 2 μM LCRed-labeled probes (final concentrations 0.2 and 0.4 μM, respectively); (v) 5.4 μl H_2O; (vi) 5 ml cDNA or pCMV-OVA solution. For the mouse β-actin cDNA measurements, samples were prepared in accordance with the instruction manuals. After an initial denaturation step at 95 °C for 10 min, temperature cycling was initiated. Each cycle consisted of denaturation at 95 °C for 10 s, hybridization at 60 °C for 15 s, and elongation at 72 °C for 10 s. The fluorescent signal was acquired at the end of the hybridization step (F2/F1 channels). The total number of cycles performed was 40. The mRNA copy numbers were calculated for each sample from the standard curve using the instrument software ('Arithmetic Fit Point analysis' for the Lightcycler). Results were expressed as relative copy numbers calculated relative to β-actin mRNA (copy number of OVA mRNA/copy number of β-actin mRNA).

Quantification of OVA mRNA in CD11c$^+$ cells after i.p. administration by quantitative PCR

pCMV-OVA (100 μg) or lipoplex was injected via the i.p. route. Spleens and peritoneal cells were harvested 6 h after i.p. administration and single cell suspensions of spleen cells were prepared in ice-cold RPMI 1640 medium. Ice-cold RPMI 1640 medium (5 ml) was injected and then peritoneal cells were collected as a cell suspension in RPMI medium. Following this, red blood cells were removed by incubation with Tris-NH_4Cl solution for 10 min at room temperature. Positive selection of CD11c$^+$ cells was carried out by magnetic cell sorting with auto MACS (Miltenyi Biotec Inc., Auburn, CA, USA) following the manufacturer's instructions. Briefly, the cell suspension was incubated with PBS containing 1 mg/ml IgG to block the Fcγ receptors of macrophages. Then, CD11c$^+$ cells were labeled by incubating with anti-CD11c monoclonal antibody (N418)-labeled magnetic beads. After washing three times, CD11c$^+$ cells were collected by auto MACS. Total RNA was isolated from the recovered CD11c$^+$ cells with a MagExtractor MFX-2000 (Toyobo Co., Ltd., Osaka, Japan) and MagExtractor-RNA following the manufacturer's instructions. Reverse transcription and quantitative PCR of OVA and β-actin mRNA were performed as described in the section 'Transfection activity by DC2.4 cells'.

Induction of OVA-specific CTL

C57BL/6 mice were immunized with naked pCMV-OVA (50 or 100 μg) or lipoplexes by i.p., i.m., or intradermal (i.d.) administration three times at intervals of 2 weeks. Two weeks after the last immunization, the spleens of each group were harvested and a single cell suspension was prepared in ice-cold RPMI 1640 medium. Then, the spleen cells were resuspended in RPMI 1640 medium supplemented with 10% FBS and 2-mercaptoethanol. The recovered spleen cells were plated in a 25-cm flask at 5×10^6 cells/ml along with MMC and E.G7-OVA cells and treated for 1 h (100 μg/ml, 1 h). Four days after cultivation, non-adherent cells were harvested, washed, and plated with relevant or irrelevant target cells at effector/target (E/T) ratios of 100 : 1, 50 : 1, 25 : 1, and 12.5 : 1. The target cells were E.G7-OVA cells or their parental cell line, EL4 cells. The target cell (E.G7-OVA or EL4 cells) suspensions in RPMI medium (2.5×10^7 cells/ml) were incubated with ^{51}Cr (7.4 MBq/ml) for 1 h. Following incubation, the cells were washed five times and then resuspended at 2×10^5 cells/ml. The target cells (E.G7-OVA or EL4 cells; 2×10^4 cells) were added to each well of a 96-well microtiter plate, along with 2×10^6, 1×10^6, 5×10^5, or 2.5×10^5 spleen cells and the plates were mixed and incubated for 4 h at 37 °C and 5% CO_2 in an incubator. After further centrifugation, 100 μl supernatant was collected from each well and the radioactivity released was measured in a gamma counter. The percentage ^{51}Cr release was calculated as follows: specific lysis (%) = [(experimental ^{51}Cr release − spontaneous ^{51}Cr release)/(maximum ^{51}Cr release − spontaneous ^{51}Cr release)] × 100). The percentage OVA-specific ^{51}Cr release was calculated as (% of ^{51}Cr release from E.G7-OVA) − (% of ^{51}Cr release from EL4).

Evaluation of protection against transplanted tumor cells in mice

C57BL/6 mice were immunized three times by i.p. or i.m. administration of naked pCMV-OVA (100 μg) or lipoplex at 2-week intervals. Then 2 weeks after the last

immunization, E.G7-OVA (1×10^6) or EL4 (1×10^6) cells were inoculated subcutaneously (s.c.) into the back of the mice. The survival of the mice was monitored up to 100 days after inoculation of the E.G7-OVA or EL4 cells.

Results

Particle sizes and zeta-potentials of Man-lipoplexes

To investigate the physicochemical properties of lipoplexes, the particle size and zeta-potential of each lipoplex were evaluated. Both lipoplexes showed a clear-cut distribution pattern and the mean particle sizes of the Man-lipoplexes and conventional lipoplex were 114 ± 7.8 and 116 ± 11.5 nm ($n = 3$), respectively. Zeta-potential analysis showed that the zeta-potential of the Man-lipoplex and the conventional lipoplex at a charge ratio (−/+) of 1.0 : 2.3 was 62.1 ± 1.85 and 64.1 ± 1.74 mV ($n = 3$), respectively. These results show that there was almost no difference in physicochemical properties between the two complexes. The galactosylated lipoplex (Gal-lipoplex) also showed a similar size distribution and zeta-potential (data not shown).

Uptake characteristics of Man-lipoplex by DC2.4 cells *in vitro*

To evaluate the potency of the Man-lipoplex in terms of targeted delivery to DCs, the uptake of the lipoplexes and subsequent transfection to cells were evaluated. In this study, we used DC2.4 cells, a cell line derived from DCs, as a model DC expressing mannose receptors [26]. The [^{32}P] Man-lipoplex was taken up by DC2.4 cells more efficiently than the conventional [^{32}P] lipoplex (Figure 1a) and this was significantly reduced in the presence of an excess of mannan (Figure 1b). In contrast, the uptake with conventional lipoplex was not significantly inhibited by an excess of mannan (Figure 1b).

Transfection characteristics of Man-lipoplex with respect to DC2.4 cells *in vitro*

We next investigated the transfection activity of the Man-lipoplex with respect to DC2.4 cells. As shown in Figure 2a, the highest gene expression was observed in the Man-lipoplex. In the presence of an excess of mannan, the gene expression of the Man-lipoplex was significantly inhibited (Figure 2b). In contrast, the gene expression with conventional lipoplex and naked pDNA was not significantly inhibited in the presence of an excess of mannan (Figure 2b).

Effect of Man-lipoplex administration routes on CTL response

To investigate the effect of the administration route of the Man-lipoplex, the induction of an OVA-specific cytotoxic response with a ^{51}Cr release assay using E.G7-OVA cells (OVA-expressing cells), and its parental cell line, EL4 cells (OVA-non-expressing cells), was examined. We found that the CTL activity induced by i.p. administration of the Man-lipoplex was higher than that induced by i.m. or i.d. administration of the Man-lipoplex (Figure 3a).

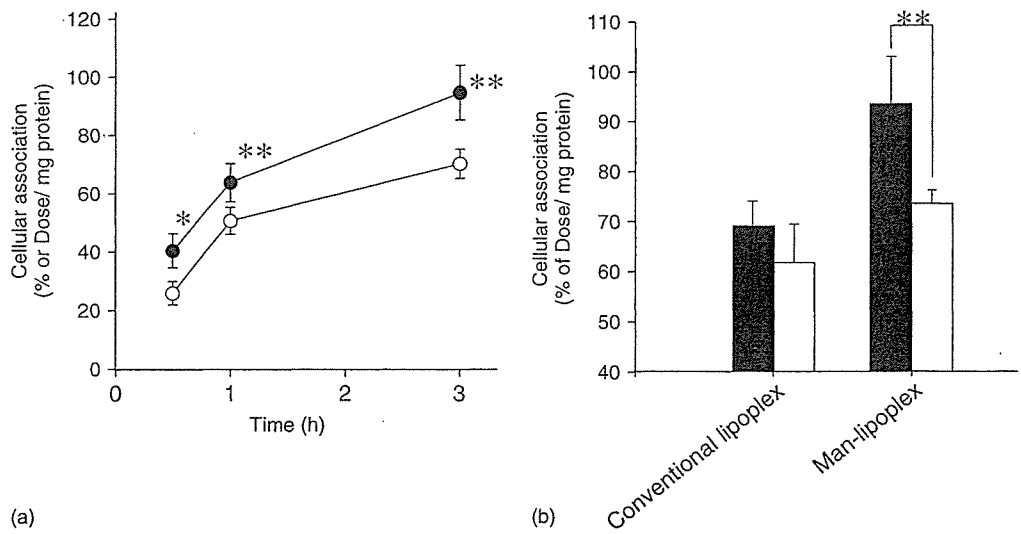

Figure 1. Cellular association of the Man-lipoplex in DC2.4 cells. (a) Cellular association time-course of ^{32}P-labeled Man-lipoplex (●) and lipoplex (○) in DC2.4 cells at 37 °C. pCMV-OVA (0.5 μg/ml) was complexed with cationic liposomes at a charge ratio (−/+) of 1.0 : 1.6. Each value represents the mean ± standard deviation (S.D.) ($n = 3$). (b) Cellular association of ^{32}P-labeled lipoplex or Man-lipoplex in the absence (■) or presence (□) of 0.125 mg/ml mannan in the culture medium. Each value represents the mean + S.D. ($n = 4$). Statistical analysis was performed by Student's *t*-test (*$P < 0.05$, **$P < 0.01$)

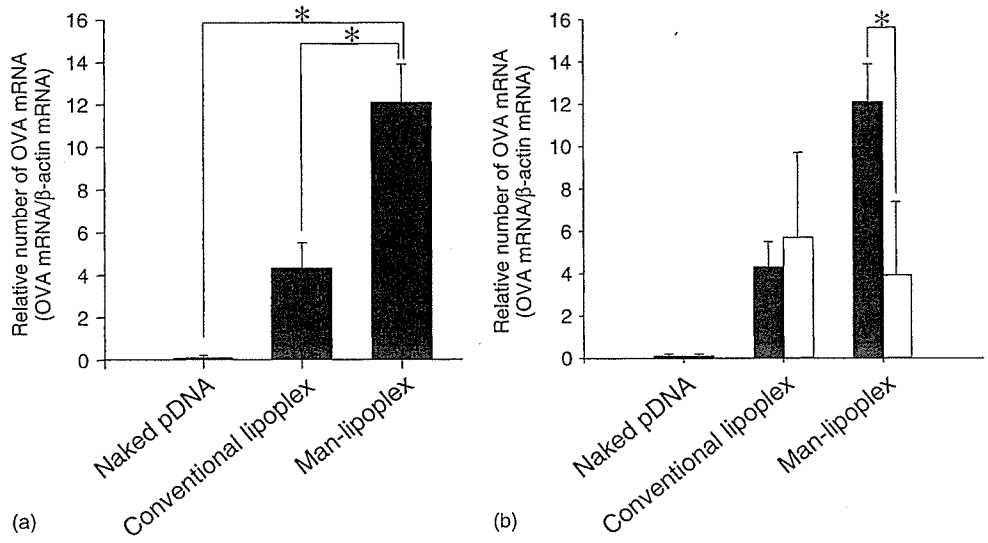

Figure 2. Transfection activity of the Man-lipoplex in DC2.4 cells. (a) Transfection activity of naked pCMV-OVA or lipoplexes in cultured DC2.4 cells. The concentration of pDNA was fixed at 0.5 μg/ml in all experiments. Each value represents the mean + S.D. (n = 3). (b) Transfection activity of naked pCMV-OVA or lipoplexes in the absence (■) or presence (□) of 0.125 mg/ml mannan. The concentration of pCMV-OVA was fixed at 0.5 μg/ml in all experiments. Each value represents the mean + S.D. values (n = 4). Statistical analysis was performed by analysis of variance (*$P < 0.05$)

Furthermore, increasing the amount of pCMV-OVA of the Man-lipoplex markedly enhanced the CTL response induced by i.p. administration (Figure 3b). Furthermore, the CTL activity of the Man-lipoplex following i.p. administration was significantly higher than that induced by i.m. administration of naked pCMV-OVA (Figure 3c).

Effect of lipoplex mannosylation on CTL response

As shown in Figure 4a, the Man-lipoplex induced a much higher CTL response than the conventional lipoplex. However, the Gal-lipoplex induced a much lower CTL response than the Man-lipoplex (Figure 4b), suggesting that the Man-lipoplex induces a strong CTL response via a mannose receptor-mediated mechanism.

Gene expression characteristics of Man-lipoplex on CD11c$^+$ cells in the spleen and peritoneal cavity after i.p. administration

To clarify the transfection activity of the Man-lipoplex with regard to DCs after i.p. administration, the OVA mRNA in the CD11c$^+$ cells in the spleen and peritoneal cavity was determined 6 h after i.p. administration of naked pCMV-OVA (100 μg) or Man-lipoplex and conventional lipoplex using quantitative RT-PCR. The relative copy number of OVA mRNA in the Man-lipoplex injected group was the highest of all in both peritoneal CD11c$^+$ cells (Figure 5a) and splenic CD11c$^+$ cells (Figure 5b).

Anti-tumor responses of Man-lipoplex after immunization

To assess the protective anti-tumor effect, EL4 and E.G7-OVA cells were transplanted into pre-immunized mice. Pre-immunization with the Man-lipoplex prolonged the survival time after transplantation of E.G7-OVA cells compared with pDNA or conventional lipoplex (Figure 6a). However, all formulations failed to prolong the survival rate after transplantation of EL4 cells (Figure 6b).

Discussion

DNA vaccine represents an exciting novel approach in vaccine development. The vaccine construct is created by insertion of a DNA encoding the desired antigen into a pDNA. The extent to which the pDNA is able to transfect cells is dependent on the application route and delivery carrier used. The encoded protein is then expressed in the transfected cells *in vivo* and, consequently, an immune response is elicited to the expressed antigen. However, to date, there have been few reports on *in vivo* gene therapy based on targeted non-viral gene delivery. In our series of experiments, we have been developing APC-selective *in vivo* gene carrier systems for use in gene therapy [22–24,32]. In the present study, we describe the Man-lipoplex given i.p. as a novel approach to enhance therapeutic potency of DNA vaccine therapy *in vivo*.

Since some clinical trials have involved the local administration of naked pDNA [7–9], we evaluated the OVA-specific CTL response following the local administration of naked pDNA. As shown in Figure 3c,

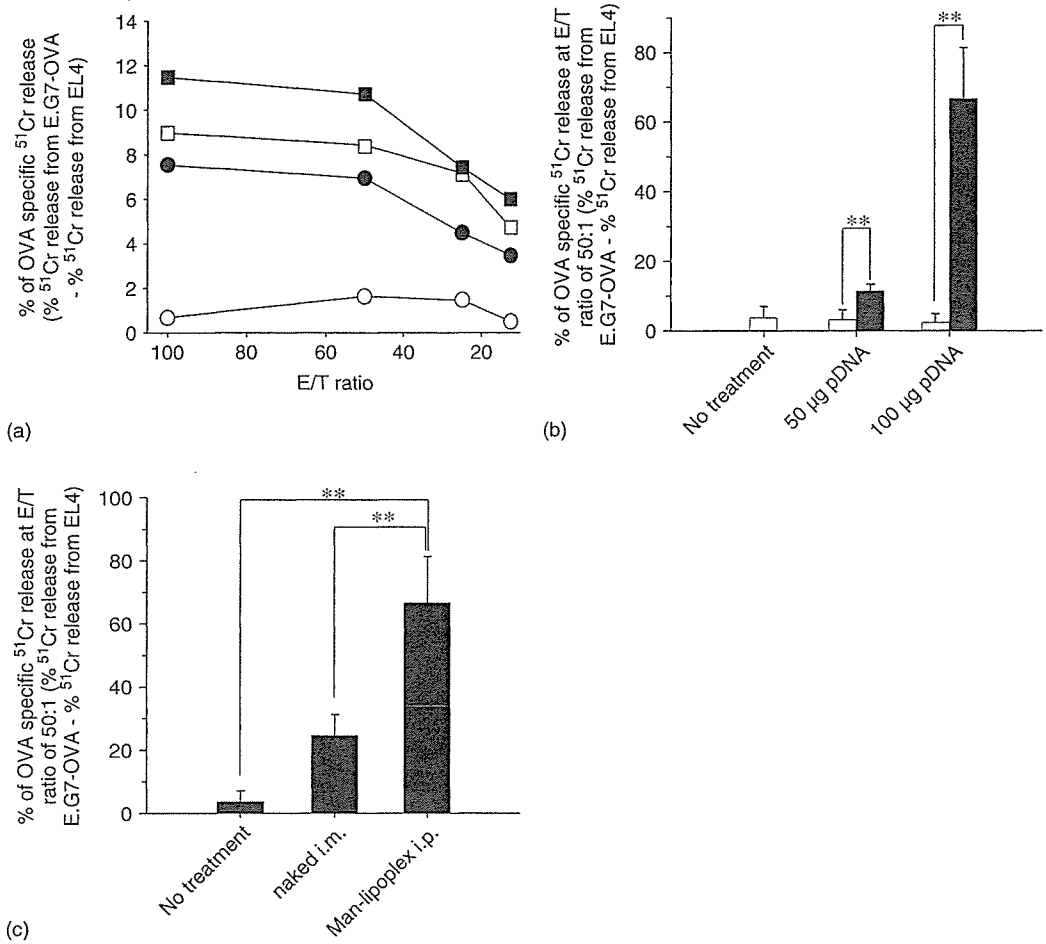

Figure 3. Effect of the route of administration and dose on immunization with naked pCMV-OVA or Man-lipoplexes. Mice were injected with 50 μg pCMV-OVA as naked pCMV-OVA or Man-lipoplexes biweekly three times before the experiment. (a) CTL activity primed by i.p. (■), i.d. (□) and i.m. (●) administration of the Man-lipoplexes or CTL activity in the no-treatment group (○). OVA-specific cell lysis at various effector/target (E/T) ratios was calculated from the % ^{51}Cr release from EL4 cells and from E.G7-OVA cells. Each value represents the mean of 4–5 experiments. (b) CTL response induced by the Man-lipoplexes (■) and naked pCMV-OVA (□) given i.p. at a dose of 50 or 100 μg/mouse. OVA-specific ^{51}Cr release at an E/T ratio of 50 : 1 was calculated from the following equation: OVA-specific ^{51}Cr release = %^{51}Cr release from E.G7-OVA cells −%^{51}Cr release from EL4 cells. Each value represents the mean + S.D. (control group: n = 3, other groups: n = 5). Statistical analysis was performed by analysis of variance (**$P < 0.01$). (c) CTL response induced by the Man-lipoplexes given i.p. and naked pCMV-OVA given i.m. at a dose of 50 or 100 μg/mouse. OVA-specific ^{51}Cr release at an E/T ratio of 50 : 1 was calculated from the following equation: OVA-specific ^{51}Cr release = %^{51}Cr release from E.G7-OVA cells −%^{51}Cr release from EL4 cells. Each value represents the mean + S.D. (control group: n = 3, other groups: n = 5). Statistical analysis was performed by analysis of variance (**$P < 0.01$)

i.p. administration of Man-lipoplex induced a higher OVA-specific CTL response than local administration of naked pDNA. To demonstrate the antigen-specific anti-tumor effects induced by vaccination, E.G7-OVA cells (OVA expressing cells), and its parent cell line, pre-immunized mice were inoculated with EL4 cells (OVA non-expressing cells). Corresponding to the CTL response, the anti-tumor effects of the Man-lipoplex were observed only in E.G7-OVA cells and the effects of the Man-lipoplex were much greater than those following local administration of naked pDNA (Figure 6). These results suggest that the Man-lipoplex is an effective gene carrier for DNA vaccination used as cancer therapy.

To demonstrate mannose receptor-mediated gene transfection of the Man-lipoplex, its transfection characteristics in DCs were evaluated in both *in vitro* and *in vivo* experiments. As shown in Figures 1 and 2, the Man-lipoplex showed significantly higher uptake and transfection activity than the conventional lipoplex and this was reduced in the presence of mannan, a mannose receptor ligand. These *in vitro* results suggest that the Man-lipoplex is taken up by mannose receptor-mediated endocytosis by a dendritic cell line, DC2.4 cells. This observation is in good agreement with our previous report showing that the Man-lipoplex is taken up by mannose receptor-mediated endocytosis by primary cultured mouse peritoneal macrophages [22,32]. To evaluate the importance of mannose receptor-mediated gene transfection to DCs, we also evaluated the involvement of the mannose receptor-mediated mechanism in the CTL response. The

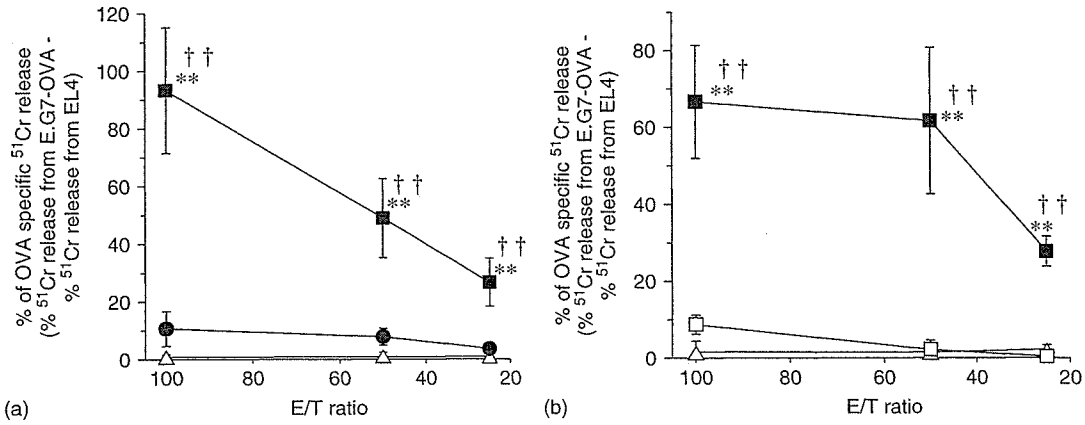

Figure 4. Effect of mannosylation of cationic liposomes on the induction of a CTL response. Mice were injected three times with naked pCMV-OVA (100 μg) or lipoplexes (pCMV-OVA; 100 μg) biweekly. (a) CTL response induced by the Man-lipoplexes (■) and the lipoplexes (●) or that of the no-treatment group (△). OVA-specific ^{51}Cr release was calculated from the following equation: OVA-specific ^{51}Cr release = %^{51}Cr release from E.G7-OVA cells −%^{51}Cr release from EL4 cells. Each value represents the mean ± S.D. (n = 4–5). (b) CTL response induced by the Man-lipoplex (■) or the Gal-lipoplex (□) or CTL response in the no-treatment group (△). OVA-specific ^{51}Cr release was calculated from the following equation: OVA-specific ^{51}Cr release = %^{51}Cr release from E.G7-OVA cells −%^{51}Cr release from EL4 cells. Each value represents the mean ± S.D. (n = 5). Statistical analysis was performed by analysis of variance. Significant difference between the no-treatment group (*$P < 0.05$, **$P < 0.01$) or pCMV-OVA given i.m. (††$P < 0.01$)

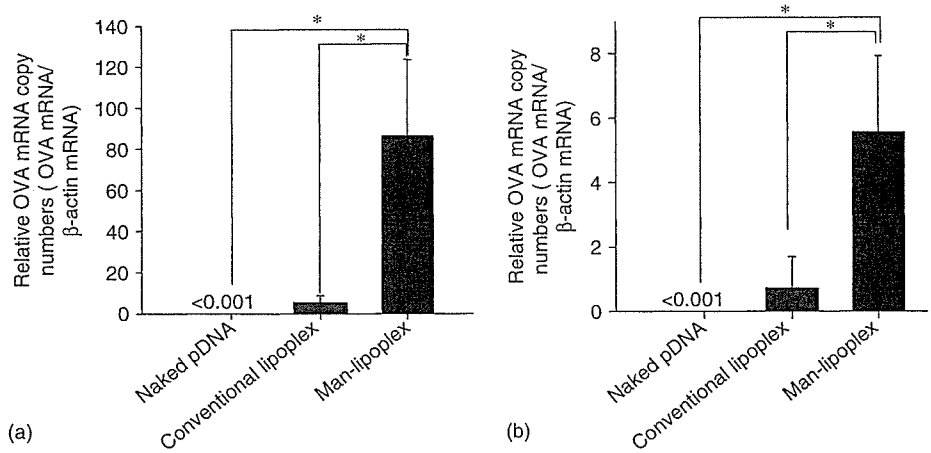

Figure 5. *In vivo* mRNA gene expression in CD11c$^+$ cells in the peritoneal cavity (a) and spleen (b) after i.p. administration to mice. Lipoplex or Man-lipoplex was prepared at a charge ratio (−/+) of 1.0 : 2.3 in 5% dextrose. Six hours after injection, OVA mRNA and β-actin mRNA eluted from CD11c$^+$ cells were measured by quantitative two-step RT-PCR. Each value represents the mean + S.D. (n = 3–4). Statistical analysis was performed by analysis of variance (*$P < 0.05$)

Gal-lipoplex was selected because it differed only from the Man-lipoplex by a sugar moiety. In a previous study, we have already confirmed that the Gal-lipoplex was taken up by asialoglycoprotein receptor-mediated endocytosis after intraportal administration [33,34]. As shown in Figure 4b, the CTL response of the Gal-lipoplex was significantly lower than that of the Man-lipoplex. These *in vitro* and *in vivo* results suggest that the Man-lipoplex is efficiently taken up by DCs via mannose receptor-mediated endocytosis.

As control cationic liposomes, cationic liposomes composed of 3β-[*N*,*N*′,*N*′-dimethylaminoethane]carbamoyl] cholesterol hydrochloride (DC-Chol liposomes) represent a feasible formulation for clinical trials involving gene therapy via the i.p. route [35] and it has also been reported that DC-Chol liposomes enhance DNA vaccine potency following i.p. administration in mice [36]. However, our preliminary experiment using pCMV-Luc demonstrated that DOTMA/Chol liposomes exhibited a much higher transfection activity than DC-Chol liposomes following i.p. administration (data not shown); therefore, DOTMA/Chol liposomes were selected as control liposomes for DNA vaccine therapy.

To further evaluate the effectiveness of lipoplex mannosylation, gene expression in APCs, OVA-specific CTL activity and the antitumor effect were compared with those obtained using conventional lipoplex. Since the lipid composition of the liposomes (DOTMA/Chol

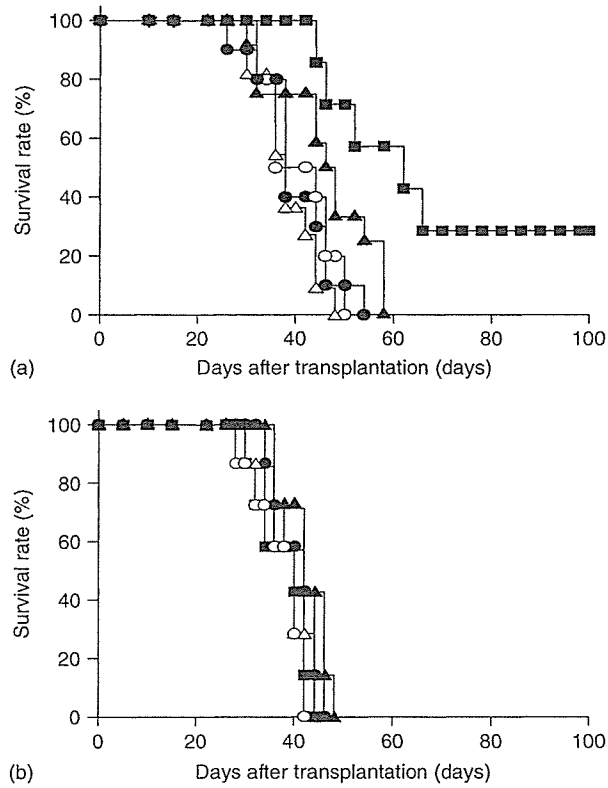

Figure 6. The anti-E.G7-OVA cell (a) or EL4 cell (b) tumor effect following pre-immunization by i.p. administration of various formulations or i.m. administration of naked pCMV-OVA solution (100 μg). Mice were injected with naked pCMV-OVA (○), the Man-lipoplex (■), or the lipoplex (●) given i.p., naked pCMV-OVA given i.m. (▲), or no treatment (△). E.G7-OVA (a) or EL4 (b) cells were transplanted into mice 2 weeks after the last immunization and the survival rate was determined (n = 7 for all groups in (b) and for Man-lipoplex in (a), n = 10 for all groups but the Man-lipoplex in (a))

vs. DOTMA/Chol/Man-C4-Chol) and the physicochemical properties (zeta-potential and particle size (see Results section)) of the lipoplex and Man-lipoplex are almost the same, the effect of mannosylation of lipoplex could be investigated by such comparisons. After i.p. administration of lipoplex or Man-lipoplex, the gene expression in $CD11c^+$ cells in the spleen and peritoneal cavity of Man-lipoplex was significantly higher than that of the conventional lipoplex (Figure 5a and 5b). Furthermore, the OVA-specific CTL response (Figure 4) and anti-tumor effect (Figure 6a) of the Man-lipoplex were significantly higher than that of the conventional lipoplex. These results convinced us that lipoplex mannosylation could enhance DNA vaccine potency.

As far as the effect of the administration route on the CTL activity by Man-lipoplex was concerned, the CTL activity following i.p. administration was higher than that following s.c. and i.m. administration (Figure 3a). We previously reported that the transfection efficiency of the lipoplex was lower than that of naked pDNA because the lipoplex is only localized at the injection site due to its cationic and macromolecular nature [37]. Thus, the lower CTL activity following s.c. and i.m. administration of the Man-lipoplex may be partly explained by our previous observation. In contrast, i.p. administrated Man-lipoplex is considered to reach the APCs in the peritoneal cavity and lymph nodes. Even the (large sized) cancer cells could distribute to the lymph nodes from the peritoneal cavity when undergoing metastasis [38,39]. Thus, these observations strongly suggest that i.p. administration is an effective administration route for gene transfection to APCs by the (Man-)lipoplex.

In the present study, we have demonstrated the effectiveness of i.p. administration of the Man-liposome formulation. This type of infusion of not only drugs such as cisplatin [42] and paclitaxel [43] but also cationic liposome/pDNA [44] has already been performed in clinical trials for ovarian cancer therapy. Regarding the i.p. administration method, implantable infusion pumps have been developed for a number of diseases [45] and there has been remarkable progress in endoscopic and laparoscopic surgical techniques [46]. These progresses in surgical techniques and devices might make i.p. administration of the Man-liposome formulation a conventional and feasible approach for the clinical application of DNA vaccine therapy.

In this study, we demonstrated that the Man-lipoplex enhanced gene expression via a mannose receptor-mediated mechanism. Since our previous study demonstrated that the Man-lipoplex were rapidly sorted from endosomes to lysosomes after uptake via mannose receptors [47], only a small part of pDNA seems to be released from endosome/lysosome to the cytosol and enters the nucleus for gene expression. Taking these findings into consideration, further modulation of intracellular sorting with some functional device should lead to more efficient gene expression in APCs. So far, functional materials such as influenza virus hemagglutinin subunit HA-2 (mHA2) [17], fusigenic peptide, and polyhistidine [48] have been grafted to the vectors to improve the intracellular sorting of cationic carrier/pDNA complexes. Modulation by grafting such functional molecules might be effective in the further development of the Man-lipoplex.

A large number of diseases can be potentially prevented or cured by DNA vaccination [40]. Recent developments in genomics technology have identified new target antigens, not only for infectious disease pathogens, but also for a large number of tumor-associated antigens [41] and this has increased the possibility of using DNA vaccines for a variety of infectious diseases and cancer therapies. Since the pDNA that encodes a variety of antigens has almost the same physicochemical properties as a polyanion, our Man-liposomes are expected to be applicable to a range of DNA vaccine therapies to enhance the CTL response.

In conclusion, we demonstrate that the Man-lipoplex produces an extremely high antigen-specific CTL response. In addition, intraperitoneal administration is an effective route for the APCs-selective gene transfection by the Man-lipoplex. Although further optimization

is required, this information will also be valuable for the future use, design, and development of a Man-lipoplex to enhance the potential of DNA vaccine therapy.

Acknowledgements

We are grateful to Dr. M. J. Bevan and Dr. K. L. Rock for providing us with pAc-neo-OVA and DC2.4 cells, respectively. This work was supported in part by Grants-in-Aid for Scientific Research from Ministry of Education, Culture, Sports, Science, and Technology of Japan, by Health and Labour Sciences Research Grants for Research on Advanced Medical Technology from the Ministry of Health, Labour and Welfare of Japan, by the Kao Foundation for Arts and Sciences, and by the Shimizu Foundation for the Promotion of Immunology Research.

References

1. Ulmer JB, Donnelly JJ, Parker SE, *et al.* Heterologous protection against influenza by injection of DNA encoding a viral protein. *Science* 1993; **259**: 1745–1749.
2. Schirmbeck R, Bohm W, Ando K, *et al.* Nucleic acid vaccination primes hepatitis B surface antigen specific cytotoxic T lymphocytes in non-responder mice. *J Virol* 1995; **69**: 5929–5934.
3. Donnelly JJ, Friedman A, Martinez D, *et al.* Preclinical efficacy of a prototype DNA vaccine: enhanced protection against antigenic drift in influenza virus. *Nat Med* 1995; **1**: 583–587.
4. Porgador A, Irvine KR, Iwasaki A, *et al.* Predominant role for directly transfected dendritic cells in antigen presentation to $CD8^+$ T cells after gene gun immunization. *J Exp Med* 1998; **188**: 1075–1082.
5. Akbari O, Panjwani N, Garcia S, *et al.* DNA vaccination: transfection and activation of dendritic cells as key events for immunity. *J Exp Med* 1999; **189**: 169–178.
6. Bot A, Stan AC, Inaba K, *et al.* Dendritic cells at a DNA vaccination site express the encoded influenza nucleoprotein and prime MHC class I-restricted cytolytic lymphocytes upon adoptive transfer. *Int Immunol* 2000; **12**: 825–832.
7. Mancini-Bourgine M, Fontaine H, Scott-Algara D, *et al.* Induction or expansion of T-cell responses by a hepatitis B DNA vaccine administered to chronic HBV carriers. *Hepatology* 2004; **40**: 874–882.
8. Rosenberg SA, Yang JC, Sherry RM, *et al.* Inability to immunize patients with metastatic melanoma using plasmid DNA encoding the gp100 melanoma-melanocyte antigen. *Hum Gene Ther* 2003; **14**: 709–714.
9. MacGregor RR, Ginsberg R, Ugen KE, *et al.* T-cell responses induced in normal volunteers immunized with a DNA-based vaccine containing HIV-1 env and rev. *AIDS* 2002; **16**: 2137–2143.
10. Arthur JF, Butterfield LH, Roth MD, *et al.* A comparison of gene transfer methods in human dendritic cells. *Cancer Gene Ther* 1997; **4**: 17–25.
11. Okada N, Tsukada Y, Nakagawa S, *et al.* Efficient gene delivery into dendritic cells by fiber-mutant adenovirus vectors. *Biochem Biophys Res Commun* 2001; **282**: 173–179.
12. Raper SE, Chirmule N, Lee FS, *et al.* Fatal systemic inflammatory response syndrome in a ornithine transcarbamylase deficient patient following adenoviral gene transfer. *Mol Genet Metab* 2003; **80**: 48–58.
13. Erbacher P, Bousser MT, Raimond J, *et al.* Gene transfer by DNA/glycosylated polylysine complexes into human blood monocyte-derived macrophages. *Hum Gene Ther* 1996; **7**: 721–729.
14. Kawakami S, Yamashita F, Nishida K, *et al.* Glycosylated cationic liposomes for cell-selective gene delivery. *Crit Rev Ther Drug Carrier Syst* 2002; **19**: 171–190.
15. Sudimack J, Lee RJ. Targeted drug delivery via the folate receptor. *Adv Drug Deliv Rev* 2000; **41**: 147–162.
16. Buning H, Ried MU, Perabo L, *et al.* Receptor targeting of adeno-associated virus vectors. *Gene Ther* 2003; **10**: 1142–1151.
17. Nishikawa M, Yamauchi M, Morimoto K, *et al.* Hepatocyte-targeted *in vivo* gene expression by intravenous injection of plasmid DNA complexed with synthetic multi-functional gene delivery system. *Gene Ther* 2000; **7**: 548–555.
18. Nishikawa M, Takemura S, Takakura Y, Hashida M. Targeted delivery of plasmid DNA to hepatocytes *in vivo*: optimization of the pharmacokinetics of plasmid DNA/galactosylated poly(L-lysine) complexes by controlling their physicochemical properties. *J Pharmacol Exp Ther* 1998; **287**: 408–415.
19. Kawakami S, Yamashita F, Nishikawa M, *et al.* Asialoglycoprotein receptor-mediated gene transfer using novel galactosylated cationic liposomes. *Biochem Biophys Res Commun* 1998; **252**: 78–83.
20. Morimoto K, Nishikawa M, Kawakami S, *et al.* Molecular weight-dependent gene transfection activity of unmodified and galactosylated polyethyleneimine on hepatoma cells and mouse liver. *Mol Ther* 2003; **7**: 254–261.
21. Nishikawa M, Takemura S, Yamashita F, *et al.* Pharmacokinetics and *in vivo* gene transfer of plasmid DNA complexed with mannosylated poly(L-lysine) in mice. *J Drug Target* 2000; **8**: 29–38.
22. Kawakami S, Sato A, Nishikawa M, *et al.* Mannose receptor-mediated gene transfer into macrophages using novel mannosylated cationic liposomes. *Gene Ther* 2000; **7**: 292–299.
23. Sato A, Kawakami S, Yamada M, *et al.* Enhanced gene transfection in macrophages using mannosylated cationic liposome-polyethylenimine-plasmid DNA complexes. *J Drug Target* 2001; **9**: 201–207.
24. Hattori Y, Kawakami S, Suzuki S, *et al.* Enhancement of immune responses by DNA vaccination through targeted gene delivery using mannosylated cationic liposome formulations following intravenous administration in mice. *Biochem Biophys Res Commun* 2004; **317**: 992–999.
25. Shen Z, Reznikoff G, Dranoff G., Rock KL. Cloned dendritic cells can present exogenous antigens on both MHC class I and class II molecules. *J Immunol* 1997; **158**: 2723–2730.
26. Cui Z, Han SJ, Huang L. Coating of mannan on LPD particles containing HPV E7 peptide significantly enhances immunity against HPV-positive tumor. *Pharm Res* 2004; **21**: 1018–1025.
27. Lee YC, Stowell CP, Krantz MJ. 2-Imino-2-methoxyethyl 1-thioglycosides: new reagents for attaching sugars to proteins. *Biochemistry* 1976; **15**: 3956–3963.
28. Moore MW, Carbone FR, Bevan MJ. Introduction of soluble protein into the class I pathway of antigen processing and presentation. *Cell* 1988; **54**: 777–785.
29. Kawakami S, Hattori Y, Lu Y, *et al.* Effect of cationic charge on receptor-mediated transfection using mannosylated cationic liposome/plasmid DNA complexes following the intravenous administration in mice. *Pharmazie* 2004; **59**: 405–408.
30. Kawakami S, Ito Y, Fumoto S, *et al.* Enhanced gene expression in lung by a stabilized lipoplex using sodium chloride for complex formation. *J Gene Med* 2005; **7**: 1526–1533.
31. Fumoto S, Kawakami S, Ito Y, *et al.* Enhanced hepatocyte-selective *in vivo* gene expression by stabilized galactosylated liposome/plasmid DNA complex using sodium chloride for complex formation. *Mol Ther* 2004; **10**: 719–729.
32. Hattori Y, Suzuki S, Kawakami S, *et al.* The role of dioleoylphosphatidylethanolamine (DOPE) in targeted gene delivery with mannosylated cationic liposomes via intravenous route. *J Control Release* 2005; **108**: 484–495.
33. Kawakami S, Fumoto S, Nishikawa M, *et al. In vivo* gene delivery to the liver using novel galactosylated cationic liposomes. *Pharm Res* 2000; **17**: 306–313.
34. Fumoto S, Nakadori F, Kawakami S, *et al.* Analysis of hepatic disposition of galactosylated cationic liposome/plasmid DNA complexes in perfused rat liver. *Pharm Res* 2003; **20**: 1452–1459.
35. Madhusudan S, Foster M, Muthuramalingam SR, *et al.* A multicenter phase I gene therapy clinical trial involving intraperitoneal administration of E1A-lipid complex in patients with recurrent epithelial ovarian cancer overexpressing HER-2/neu oncogene. *Clin Cancer Res* 2004; **10**: 2986–2996.
36. Ishii N, Fukushima J, Kaneko T, *et al.* Cationic liposomes are a strong adjuvant for a DNA vaccine of human immunodeficiency virus type 1. *AIDS Res Hum Retroviruses* 1997; **13**: 1421–1428.
37. Nomura T, Nakajima S, Kawabata K, *et al.* Intratumoral pharmacokinetics and *in vivo* gene expression of naked plasmid DNA and its cationic liposome complexes after direct gene transfer. *Cancer Res* 1997; **57**: 2681–2686.

38. Dubernard G, Morice P, Rey A, *et al.* Lymph node spread in stage III or IV primary peritoneal serous papillarycarcinoma. *Gynecol Oncol* 2005; 97: 136–141.
39. Dullens HF, Rademakers LH, Cluistra S, *et al.* Parathymic lymph nodes during growth and rejection of intraperitoneally inoculated tumor cells. *Invasion Metastasis* 1991; **11**: 216–226.
40. Donnelly JJ, Ulmer JB, Shiver JW, Liu MA. DNA vaccines. *Annu Rev Immunol* 1997; **15**: 617–648.
41. Polo JM, Dubensky TW Jr. Virus-based vectors for human vaccine applications. *Drug Discov Today* 2002; 7: 719–727.
42. Sabbatini P, Aghajanian C, Leitao M, *et al.* Intraperitoneal cisplatin with intraperitoneal gemcitabine in patients with epithelial ovarian cancer: results of a phase I/II trial. *Clin Cancer Res* 2004; **10**: 2962–2967.
43. Gelderblom H, Verweij J, van Zomeren DM, *et al.* Influence of Cremophor El on the bioavailability of intraperitoneal paclitaxel. *Clin Cancer Res* 2000; 8: 1237–1241.
44. Madhusudan S, Tamir A, Bates N, *et al.* A multicenter phase I gene therapy clinical trial involving intraperitoneal administration of E1A-lipid complex in patients with recurrent epithelial ovarian cancer overexpressing HER-2/neu oncogene. *Clin. Cancer Res* 2004; **10**: 2986–2996.
45. Hepp KD. Implantable insulin pumps and metabolic control. *Diabetologia* 1994; **37**: S108–S111.
46. Stellato TA. History of laparoscopic surgery. *Surg Clin North Am* 1992; **72**: 997–1002.
47. Yamada M, Nishikawa M, Kawakami S, *et al.* Tissue and intrahepatic distribution and subcellular localization of a mannosylated lipoplex after intravenous administration in mice. *J Control Release* 2004; **98**: 157–167.
48. Midoux P, Kichler A, Boutin V, *et al.* Membrane permeabilization and efficient gene transfer by a peptide containing several histidines. *Bioconjugate Chem* 1998; **9**: 260–267.

Department of Drug Delivery Research, Graduate School of Pharmaceutical Sciences, Kyoto University, Kyoto, Japan

Suppression of TNFα production in LPS induced liver failure in mice after intravenous injection of cationic liposomes/NFκB decoy complex

Y. Higuchi, S. Kawakami, M. Oka, F. Yamashita, M. Hashida

Received August 8, 2005, accepted September 6, 2005

Prof. Mitsuru Hashida, Department of Drug Delivery Research, Graduate School of Pharmaceutical Sciences, Kyoto University, Sakyo-ku, Kyoto 606-8501, Japan.
hashidam@pharm.kyoto-u.ac.jp

Pharmazie 61: 144–147 (2006)

NFκB decoy, double stranded oligonucleotides containing NFκB binding sequences, inhibits NFκB-mediated production of inflammatory cytokines, and therefore NFκB decoy has been applied to several diseases. However, naked NFκB decoy, which is quickly cleared from the circulation in mice after intravenous injection, is readily absorbed into the systemic circulation. In order to deliver enough NFκB decoy for a therapeutic effect, it is necessary to develop a carrier, which enables much more NFκB decoy to transfer to the target cells. In this study, using *N*-[1-(2,3-dioleyloxy)propyl]-*n,n,n*-trimethylammonium chloride (DOTMA)/cholesterol (1 : 1) liposomes, the therapeutic effect of NFκB decoy was investigated in an LPS induced acute hepatitis model mice. The mean diameter of the cationic liposomes/NFκB decoy complex was about 70.9 nm and the zeta potential of complex was about 37.4 mV. Tissue distribution was determined by measuring the radioactivity of a cationic liposomes/[^{32}P] NFκB decoy complex after intravenous injection. The cationic liposomes/[^{32}P] NFκB decoy complex was rapidly accumulated in the lung and gradually moved to the liver. The therapeutic effect was determined by the serum concentration of TNFα in LPS treated mice. The production of TNFα was significantly inhibited by cationic liposomes/NFκB decoy complex but not by cationic liposomes/random decoy complex or naked NFκB decoy. These results suggested that NFκB decoy therapy could be achieved using cationic liposomes. This information is of great value for the design of NFκB decoy carrier systems.

1. Introduction

Endotoxin syndrome is a particularly serious complication because bacteriologically proven infection occurs in up to 80% of patients with hepatic failure (Rolando et al. 1990, 2000). Binding of lipopolysaccharide (LPS) by toll-like receptor 4 expressed on macrophages causes the activation of transcriptional factor nuclear factor kappa B (NFκB), triggering the rapid release of cytokines TNFα, IL-1, IL-2, IL-6, IL-8, IL-12, and IFN-β, etc. by macrophages (Morrison et al. 1987; Heinzel, 1990; Dinarello et al. 1993; Essani et al. 1996; Pahl et al. 1999; Han et al. 2002). Therefore, prevention of NFκB activation would be a critical therapeutic goal of fetal liver injury caused by the endotoxin syndrome. Several recent reports indicate that NFκB decoy, double stranded oligonucleotides containing NFκB binding sequences, inhibits NFκB-mediated production of inflammatory cytokines (Morishita et al. 1997, Tomita et al. 2000a); therefore, NFκB decoy could be used in various diseases (Tomita et al. 2000, Yoshimura et al. 2001, Azuma et al. 2003). Considering that naked NFκB decoy is easily digested by DNase in serum and hardly taken up by cells, it is necessary to develop a non-invasive form of NFκB decoy delivery, which would be safe for repeated use and provide reproducible therapeutic effects, for wider clinical application.

In spite of the high transfection efficiency of viral vectors, safety concerns have been raised in clinical trials because of their highly toxic nature; therefore, the use of non-viral vectors has attracted great interest for *in vivo* gene delivery because they are free from some of the risks inherent in these systems (Mahato et al. 1997; Kawakami et al. 2002; Hashida et al. 2005). We previously reported that rapid clearance of pDNA from the circulation was observed with extensive accumulation in the lung and liver after intravenous injection of pDNA complexed with cationic liposomes (Mahato et al. 1995a, 1995b). As regards intrahepatic distribution, pDNA complexed with cationic liposomes was predominantly taken up by liver non-parenchymal cell (NPC), composed of Kupffer cells, sinusoidal endothelial cells etc., via a phagocytic process. NFκB decoy is a double stranded oligonucleotide which could interact with cationic liposomes. Because NPC is a main target for NFκB decoy inhibition of NFκB-mediated production of inflammatory cytokines, it would be expected that NFκB decoy delivery to liver NPC by cationic liposomes would efficiently suppress cytokine production by the prevention of NFκB activation. However, little information is available on the use of cationic liposomes/NFκB decoy complex against inflammatory disease after intravenous administration.

In this study, the physicochemical properties and distribution characteristics of a NFκB decoy/cationic liposomes complex were evaluated. In mice with LPS induced hepatitis, TNFα concentration was measured to evaluate the prevention of NFκB activation after intravenous administration of NFκB decoy/cationic liposomes complex. *N*-[1-(2,3-dioleyloxy)propyl]-*n*,*n*,*n*-trimethylammonium chloride (DOTMA)/cholesterol (1 : 1) liposomes were selected as the cationic liposomes because of the many reports about their use for *in vivo* pDNA delivery with high transfection efficacy (Song et al. 1997; Kawakami et al. 2000, 2001). Results were compared with naked NFκB decoy.

2. Investigations, results and discussion

The table summarizes data on mean diameter and zeta potential of cationic liposomes and the cationic liposomes/NFκB decoy complex. It has been reported that mixing complexes at low ion strength prevents aggregation, although large complexes resulting from aggregation showed high transfection efficiency *in vitro* in the case of DNA/transferring-PEI complexes (Ogris et al. 1998). Having regard to this report, the cationic liposomes/NFκB decoy complexes were prepared with 5% dextrose solution. The mean diameter of the cationic liposomes or cationic liposomes/NFκB decoy complex was about 73.8 and 70.9 nm, respectively. There was no significant difference in the mean diameter of empty liposomes and complex.

The zeta potential of cationic liposomes or cationic liposomes/NFκB decoy complex was about 56.7 and 37.4 mV, respectively. The zeta potential of the cationic liposomes/NFκB decoy complex was slightly smaller than that of empty liposomes. This result suggested that NFκB decoy would form a complex with cationic liposomes because attaching NFκB decoy with anionic charge to cationic liposomes would decrease the zeta potential of the cationic liposomes.

The liver and lung accumulation of the cationic liposomes/[^{32}P] NFκB decoy complex was compared with that of naked [^{32}P] NFκB decoy (Fig. 1). Both liver and lung accumulation of the cationic liposomes/[^{32}P] NFκB decoy complex were significantly higher than for naked [^{32}P] NFκB decoy at 1, 10, and 60 min after injection. Focusing on the cationic liposomes/[^{32}P] NFκB decoy complex, the complex accumulated initially in the lung at 1 min after injection, then moved gradually to the liver. At 60 min, 60% of the dose of the cationic liposomes/[^{32}P] NFκB decoy complex had accumulated in the liver (Fig. 1B). In our previous study, we demonstrated that [^{32}P] pDNA complexed with DOTMA/cholesterol liposomes rapidly accumulated in the lung and gradually accumulated in the liver (Mahato et al. 1995a, 1995b). Our findings concur that distribution of the cationic liposomes/NFκB decoy complex agrees with the distribution of the cationic liposomes/pDNA complex.

In order to determine the therapeutic effect of NFκB decoy on acute hepatitis *in vivo*, the serum concentration of TNFα in LPS treated mice was measured after intravenous injection of NFκB decoy (Fig. 2). Cationic liposomes/NFκB decoy complex suppressed the increase of TNFα in the serum, although naked NFκB decoy did not show an inhibitory effect on the production of TNFα. In endotoxin-induced liver failure, it is known that Kupffer cells, resident macrophages in the liver, play a major role in producing inflammatory cytokines (Arai et al. 1993; Iimuro et al. 1994; Mochida et al. 1996). Considering that the liver accumulation of the cationic liposomes/NFκB decoy complex was significantly higher than that of naked NFκB decoy (Fig. 1), this raises the possibility that some part of the NFκB decoy taken up by Kupffer cell might suppress NFκB mediated TNFα production induced by LPS.

To examine whether the inhibitory effect of NFκB decoy depended on the sequence of NFκB binding site, a similar size of double stranded oligonucleotide without NFκB binding site and also without any effective sequence, which was called random decoy, was designed and the inhibitory effect of its complex with cationic liposomes on TNFα production investigated. As shown in Fig. 2, the cationic liposomes/random decoy complex had no effect on TNFα production; therefore, the inhibitory effect on TNFα production was observed to depend on the sequence of NFκB decoy.

To determine the effect of dose of NFκB decoy, the inhibitory effect on LPS induced TNFα production in serum was investigated at different doses of NFκB decoy com-

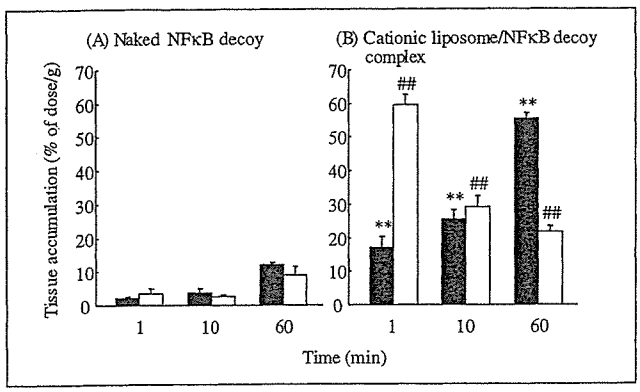

Fig. 1: Tissue accumulation of naked [^{32}P] NFκB decoy (A) or cationic liposomes/[^{32}P] NFκB decoy complex (B) after intravenous injection into mice. Radioactivity was determined in liver (■) and lung (□). Each value represents the mean + S.D. (n = 3). Significant difference ** $P < 0.01$ vs. liver accumulation of naked NFκB decoy and ## $P < 0.01$ vs. lung accumulation of naked NFκB decoy

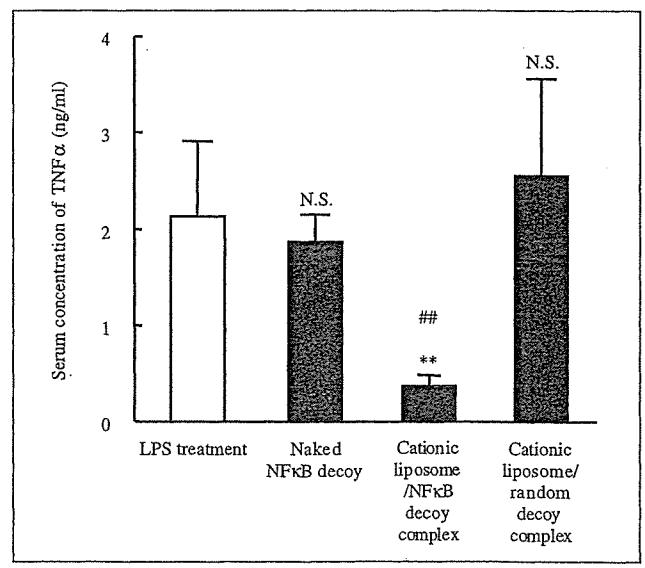

Fig. 2: Effect of complex formation and sequence of NFκB decoy on prevention of the TNFα production after intravenous injection of naked NFκB decoy, cationic liposomes/NFκB decoy complex or cationic liposomes/random decoy complex into mice. Each value represents the mean + S.D. (n = 3). Significant difference ** $P < 0.01$ vs. naked NFκB decoy, ## $P < 0.01$ vs. random decoy complex and N.S. not significant

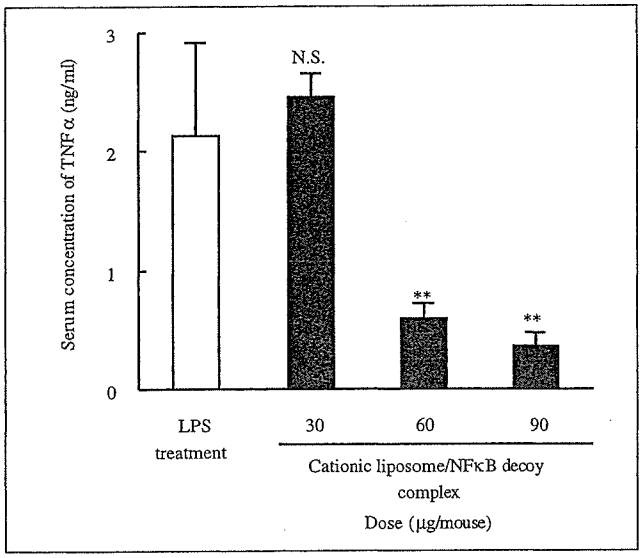

Fig. 3: Effect of dose on the prevention of TNFα production after intravenous injection of cationic liposomes/NFκB decoy complex into mice. Each value represents the mean + S.D. (n = 3). Significant difference ** $P < 0.01$ vs LPS treatment and N.S. not significant

plexed with cationic liposomes (Fig. 3). At doses of 60 and 90 μg/mouse, the production of TNFα was significantly inhibited but not at 30 μg/mouse.

To date, several kinds of non-viral carriers have been applied to *in vivo* gene delivery. As far as NFκB decoy delivery targeting to the liver is concerned, Ogushi et al. (2003) have also demonstrated the inhibitory effect of NFκB decoy on the production of cytokines using HVJ liposomes given by intraportal injection. HVJ liposomes are well known as a gene carrier, which could rapidly fuse to cells and transfer the incorporated gene to the cells. However, HVJ liposomes are not suitable for intravenous injection because intravenously injected HVJ liposomes accumulate in the lung, spleen, kidney and liver; therefore, several researchers have reported that they could not achieve enough therapeutic effect or transfection efficiency (Hirano et al. 1998; Morishita et al. 2000; Yoshida et al. 2002; Ogushi et al. 2003). Conversely, we report here that intravenously injected cationic liposomes/NFκB decoy complex accumulates in the liver (Fig. 1).

Cationic liposome-based systemic pDNA delivery has been reported as a novel technology, however the uptake of cationic liposomes/pDNA by Kupffer cells triggers production of inflammatory cytokines and disturbs gene transfer efficiency, which is largely due to unmethylated CpG motif in the pDNA (Sakurai et al. 2002). Recently, Tan et al. have reported that NFκB decoy could inhibit TNFα induction by a cationic liposomes (DOTAP/cholesterol, 1 : 1)/pDNA complex, which was prepared by mixing liposome solution and DNA solution containing pDNA and NFκB decoy (Tan et al. 2002). In this study, we demonstrate that LPS induced TNFa production could be inhibited by cationic liposomes/NFκB decoy complex (Fig. 2). This result leads us to believe that the cationic liposomes/NFκB decoy complex in liver is mainly distributed in Kupffer cells after intravenous injection.

In this study, we demonstrate that intravenously injected cationic liposomes/NFκB decoy complex effectively inhibits TNFα production in LPS induced acute hepatitis in mice. This result will give useful information on NFκB decoy therapy using cationic liposomes. With more study and development of cellular targeting with cationic liposomes, it will be possible to establish NFκB therapy by intravenous injection.

Table: Mean particle sizes and zeta potentials of cationic liposomes and cationic liposomes/NFκB decoy complexes

	Particle size (nm)	Zeta potential (mV)
Cationic liposome	73.8 ± 5.46	56.7 ± 1.53
Cationic liposome/NFκB decoy complex	70.9 ± 1.07	37.4 ± 2.84

Results are expressed as the mean ± SD of three experiments

3. Experimental

3.1. Materials

NFκB decoy and control oligonucleotides used in this study are phosphodiester double stranded oligonucleotides. Their sequences are as follows: 20 mer NFκB decoy 5′-AGTTGAGGGGACTTTCCCAGGC-3′ 5′-TCAACTCCCCTGAAAGGGTCCG-3′ (B), control oligonucleotides 5′-TTGCCGTACCTGACTTAGCC-3′ 5′-AACGGCATGGACTGAATCGG-5′. These oligonucleotides were purchased from Operon Biotechnologies, Inc. (Tokyo, Japan). DOTMA was obtained from Tokyo Kasei Kogyo Co., Ltd. (Tokyo, Japan). Cholesterol, Clear-Sol I and Soluen 350 were obtained from Nacalai Tesque Inc. (Kyoto, Japan). Lipopolysaccharide (LPS) from Salmonella Minnesota Re 595 (Re mutant) was purchased from Sigma Chemicals Inc. (St. Louis, MO, USA). [γ-^{32}P] ATP and NAP 5^{TM} columns were purchased from Amersham Biosciences Corp. (Piscataway, NJ, USA). MEGALABELTM 5′-End Labeling Kit was purchased from Takara Bio Inc. (Shiga, Japan). OptiEIA^{TM} enzyme-linked immuno-sorbent assay (ELISA) kit (BD Biosciences, San Jose, CA, USA). Enzyme Immunoassay for NFκB Product No.TF 01 was purchased from Oxford Biomedical Research, Inc. (Oxford, MI, USA). All other chemicals were of the highest purity available.

3.2. Preparation of liposomes

DOTMA was mixed with cholesterol, each in chloroform at a molar ratio of 1 : 1 and the mixture was dried, vacuum desiccated, and resuspended in sterile 5% dextrose. After hydration, the dispersion was sonicated for 10 min in a bath sonicator and then for 3 min in a tip sonicator to form liposomes. The preparation method for liposomes/NFκB decoy complexes for *in vivo* use has been reported previously (Kawakami et al., 2000b, 2004). Briefly, equal volumes of NFκB decoy and stock liposome solution diluted with 5% dextrose to produce various ratios of liposomes/NFκB decoy were mixed in 1.5 ml tubes at room temperature. Then, the NFκB decoy solution was added rapidly to the liposomes solution using a Pipetman pipet and the mixture was agitated rapidly by pumping it up and down twice in the pipet tip. The mixing ratio of liposomes and NFκB decoy was expressed as a +/− charge ratio, which is the molar ratio of cationic lipids to NFκB decoy phosphate residue (Huang et al. 1997).

3.3. Measurement of particle size and zeta potentials

The mean diameters of cationic liposomes or cationic liposomes/NFκB decoy complex were measured by dynamic light-scattering spectrophotometric methods using an LS-900 (Otsuka Electronics, Osaka, Japan). The zeta potentials of cationic liposomes or cationic liposomes/NFκB decoy complex were measured by laser-Doppler electrophoresis using a Zetasizer Nano ZS (Malvern Instruments Ltd, Worcestershire, UK).

3.4. Radiophosphorylation of decoy oligonucleotides

Oligonucleotides were labeled with [γ-^{32}P] ATP using a MEGALABELTM 5′-End Labeling Kit. Briefly, oligonucleotides, [γ-^{32}P] ATP and T4 polynucleotide kinase were mixed in phosphorylation buffer. After 30 min incubation at 37 °C, the mixture was incubated for 10 min at 70 °C in order to inactivate T4 polynucleotide kinase. Then, the mixture was purified by gel chromatography using a NAP 5^{TM} column and eluted with 10 mM Tris-Cl and 1 mM EDTA (pH 8.0). The fractions containing derivatives were selected on the basis of their radioactivity.

3.5. In vivo distribution

[^{32}P] NFκB (20 μg) decoy complexed with liposomes in 300 μl of 5% dextrose solution was injected intravenously to female five-week-old ICR mice (19–22 g). The mice were killed at 1, 10 and 60 min. Liver and lung were removed, washed with saline, blotted dry, and weighed. A small amount of each tissue was digested with 0.7 ml of Soluene-350 by incuba-

tion overnight at 54 °C. Following digestion, 0.2 ml isopropanol, 0.2 ml 30% hydrogen peroxide, 0.1 ml 5N HCl, and 5.0 ml Clear-Sol I were added. The samples were stored overnight, and radioactivity was measured in a scintillation counter (LSA-500, Beckman, Tokyo, Japan).

3.6. Cytokine secretion

Mice were purchased from Shizuoka Agricultural Cooperative Association for Laboratory Animals (Shizuoka, Japan). All animal experiments were carried out in accordance with the Principles of Laboratory Animal Care as adopted and promulgated by the US National Institutes of Health and the Guidelines for Animal Experiments of Kyoto University. The indicated amount of NFκB decoy or random decoy complexed with liposomes or the indicated amount of naked NFκB decoy in 300 μl of 5% dextrose solution was intravenously injected to the mice. Blood was collected from the mice 1 h after intravenous injection of LPS. The blood was allowed to coagulate for 3 h at 4 °C and serum was isolated as the supernatant fraction following centrifugation at 17000 × g for 20 min. The serum samples were immediately stored at −80 °C. The amounts of TNFα were analyzed using an OptiEIA™ ELISA kit according to the manufacturer's protocol.

3.7. Statistical analysis

Statistical comparisons were performed by Student's t test for two groups, one-way ANOVA for multiple groups, and Scheffe's post hoc test after ANOVA.

Acknowledgement: This work was supported in part by Grants-in-Aids for Scientific Research from the Ministry of Education, Culture, Sports, Science, and Technology of Japan, and by Health and Labor Sciences Research Grants for Research on Advanced Medical Technology from the Ministry of Health, Labor and Welfare of Japan.

This research paper was presented during the 5th Conference on Retrometabolism-Based Drug Design and Targeting, May 8–11, 2005, Hakone, Japan.

References

Arai M, Mochida S, Ohno A, Ogata I, Fujiwara K (1993) Sinusoidal endothelial cell damage by activated macrophages in rat liver necrosis. Gastroenterology 104: 1466–1471.

Azuma H, Tomita N, Kaneda Y, Koike H, Ogihara T, Katsuoka Y, Morishita R (2003) Transfection of NFκB-decoy oligodeoxynucleotides using efficient ultrasound-mediated gene transfer into donor kidneys prolonged survival of rat renal allografts. Gene Ther 10: 415–425.

Dinarello CA, Gelfand JA, Wolff SM (1993) Anticytokine strategies in the treatment of the systemic inflammatory response syndrome. JAMA 269: 1829–1835.

Essani NA, McGuire GM, Manning AM, Jaeschke H (1996) Endotoxin-induced activation of the nuclear transcription factor κB and ezpression of E-selectin messenger RNA in hepatocytes, Kupffer cells, and endothelial cells *in vivo*. J Immunol 156: 2956–2963.

Han SJ, Ko HM, Cho JH, Seo KH, Lee HS, Choi EK, Choi IW, Lee HK, Im SY (2002) Molecular mechanism for lipopolysaccharide-induced biphasic activation of nuclear factor-κB. J Biol Chem 277: 44715–44721.

Hashida M, Kawakami S, Yamashita F (2005) Lipid carrier systems for targeted drug and gene delivery. Chem Pharm Bull, 53: 871–880.

Heinzel FP (1990) The role of IFN-γ in the pathology of experimental endotoxemia. J Immunol 145: 2920–2924.

Hirano T, Fujimoto J, Ueki T, Yamamoto H, Iwasaki T, Morisita R, Sawa Y, Kaneda Y, Takahashi H, Okamoto E (1998) Persistent gene expression in rat liver *in vivo* by repetitive transfections using HVJ-liposome. Gene Ther 5: 459–464.

Huang LS (1997) *In vivo* gene transfer via intravenous administration of cationic lipid-protamine DNA (LPD) complexes. Gene Ther 4: 891–900.

Iimuro Y, Yamamoto M, Kohno H, Itakura J, Fujii H, Matsumoto Y (1994) Blockade of liver macrophages by gadolinium chloride reduces lethality in endotoxemic rats–analysis of mechanisms of lethality in endotoxemia. J Leukoc Biol 55: 723–728.

Kawakami S, Fumoto S, Nishikawa M, Yamashita F, Hashida M (2000a) *In vivo* gene delivery to the liver using novel galactosylated cationic liposomes. Pharm Res 17: 306–313.

Kawakami S, Wong J, Sato A, Hattori Y, Yamashita F, Hashida M (2000b) Biodistribution characteristics of mannosylated, fucosylated, and galactosylated liposomes in mice. Biochim Biophys Aca 1524: 258–265.

Kawakami S, Sato A, Yamada M, Yamashita F, Hashida M (2001) The effect of lipid composition on receptor-mediated *in vivo* gene transfection using mannosylated cationic liposome in mice. STP Pharma Sci 11: 117–120.

Kawakami S, Yamashita F, Nishida K, Nakamura J, Hashida M (2002) Glycosylated cationic liposomes for cell-selective gene delivery. Crit Rev Ther Drug Carrier Syst 19: 171–190.

Kawakami S, Hattori Y, Lu Y, Higuchi Y, Yamashita F, Hashida M (2004) Effect of cationic charge on receptor-mediated transfection using mannosylated cationic liposome/plasmid DNA complexes following the intravenous administration in mice. Pharmazie 59: 405–408.

Mahato RI, Kawabata K, Nomura T, Takakura Y, Hashida M (1995a) Physicochemical and pharmacokinetic characteristics of plasmid DNA/cationic liposome complexes. J Pharm Sci 84: 1267–1271.

Mahato RI, Kawabata K, Takakura Y, Hashida M (1995b) *In vivo* disposition characteristics of plasmid DNA complexed with cationic liposomes. J Drug Target 3: 149–157.

Mahato RI, Takakura Y, Hashida M (1997) Nonviral vectors for *in vivo* gene delivery: physicochemical and pharmacokinetic considerations. Crit Rev Ther Drug Carrier Syst 14: 133–172.

Mochida S, Ohno A, Arai M, Tamatani T, Miyasaka M, Fujiwara K (1996) Role of adhesion molecules in the development of massive hepatic necrosis in rats. Hepatology 23: 320–328.

Morishita R, Sugimoto T, Aoki M, Kida I, Tomita N, Moriguchi A, Maeda K et al. (1997) In vivo transduction of cis element decoy against nuclear factor-κB binding site prevents myocardial infarction. Nat Med 3: 894–899.

Morishita R, Gibbons GH, Kaneda Y, Ogihara T, Dzau VJ (2000) Systemic administration of HVJ viral coat-liposome complex containing human insulin vector decreases glucose level in diabetic mouse: a model of gene therapy. Biochem Biophys Res Commun 273: 666–674.

Morrison DC, Ryan JL (1987) Endotoxins and disease mechanisms. Annu Rev Med 38: 417–432.

Ogris M, Steinlein P, Kursa M, Mechtler K, Kircheis R, Wagner E (1998) The size of DNA/transferrin-PEI complexes is an important factor for gene expression in cultured cells. Gene Ther 5: 1425–1433.

Ogushi I, Iimuro Y, Seki E, Son G, Hirano T, Hada T, Tsutsui H, Nakanishi K, Morishita R, Kaneda Y, Fujimoto J (2003) Nuclear factor κB decoy oligonucleotides prevent endotoxin-induced fatal liver failure in a murine model. Hepatology 38: 335–344.

Pahl HL (1999) Activations and target genes of Rel/NF-κB transcription factors. Oncogene 18: 6853–6866.

Rolando N, Harvey F, Brhm J, Philpott-Howars J, Alexander G, Gimson A, Casewell M (1990) Prospective study of bacterial infection in acute liver failure: an analysis of fifty patients. Hepatology 11: 49–53.

Roland N, Wade J, Davalos M, Wendon J, Philpott-Howars J, Williams R (2000) The system inflammatory response syndrome in acute liver failure. Hepatology 32: 734–739.

Sakurai F, Terada T, Yasuda K, Yamashita F, Takakura Y, Hashida M (2002) The role of tissue macrophages in the induction of proinflammatory cytokine production following intravenous injection of lipoplexes. Gene Ther 9: 1120–1126.

Song YK, Liu F, Chu S, Liu D (1997) Characterization of cationic liposome-mediated gene transfer *in vivo* by intravenous administration. Hum Gene Ther 8: 1585–1594.

Tan Y, Zhang JS, Huang L (2002) Codelivery of NF-κB decoy-related oligodeoxynucleotide improves LPD-mediated systemic gene transfer Mol Ther 6: 804–812.

Tomita N, Morishita R, Tomita S, Gibbons GH, Zhang L, Horiuchi M, Kaneda Y, Higaki J, Ogihara T, Dzau VJ (2000) Transcription factor decoy for NF kappa B inhibits TNFα induced cytokine and adhesion molecule molecule expression in vivo. Gene Ther 7: 1326–1332.

Yoshida M, Yamamoto N, Uehara T, Terao R, Nitta T, Harada N, Hatano E, Iimuro Y, Yamaoka Y (2002) Kupffer cell targeting by intraportal injection of the HVJ cationic liposome. Eur Surg Res 34: 251–259.

Yoshimura S, Morishita R, Hayashi K, Yamamoto K, Nakagami H, Kaneda Y, Sakai N, Ogihara T (2001) Inhibition of intimal hyperplasia after balloon injury in rat carotid artery model using cis-element 'decoy' of nuclear factor-κB binding site as a novel molecular strategy. Gene Ther 8: 1635–1642.

0022-3565/05/3152-484–493$20.00
THE JOURNAL OF PHARMACOLOGY AND EXPERIMENTAL THERAPEUTICS

JPET 315:484–493, 2005

Vol. 315, No. 2
89516/3054856
Printed in U.S.A.

Interaction with Blood Components Plays a Crucial Role in Asialoglycoprotein Receptor-Mediated in Vivo Gene Transfer by Galactosylated Lipoplex

Shintaro Fumoto, Shigeru Kawakami, Kosuke Shigeta, Yuriko Higuchi, Fumiyoshi Yamashita, and Mitsuru Hashida

Department of Drug Delivery Research, Graduate School of Pharmaceutical Sciences, Kyoto University, Kyoto, Japan

Received May 13, 2005; accepted July 19, 2005

ABSTRACT

In this study, we evaluated the effect of blood components (whole blood and serum) on asialoglycoprotein receptor-mediated in vivo gene transfer. The hepatic transfection activity of galactosylated lipoplex preincubated with serum was approximately 10 times higher than that without incubation after intraportal injection in mice. However, preincubation with whole blood significantly reduced hepatic transfection activity. Fluorescent resonance energy transfer analysis and agarose gel electrophoresis revealed that preincubation with serum reduced the degree of destabilization of the galactosylated lipoplex in blood, partially supporting enhanced hepatic transfection activity by preincubation with serum. Inhibition of hepatic transfection activity by predosing galactosylated bovine serum albumin indicated that the galactosylated lipoplex exposed to serum is recognized by asialoglycoprotein-receptors on hepatocytes. Inactivation of serum prior to mixing with galactosylated lipoplex reduced liver accumulation and completely abolished enhancement of hepatic transfection activity by preincubation with active serum, suggesting that not only the stability of the lipoplex in blood but also the serum opsonin activity plays important roles. Alternatively, preincubation with inactivated serum reduced the lung accumulation and inflammatory cytokine production of galactosylated lipoplex. The information provided by this study will be valuable for the future use, design, and development of galactosylated lipoplex for in vivo asialoglycoprotein receptor-mediated gene transfer.

For effective and safe in vivo gene transfer, the development of targeted gene delivery systems is a promising approach. To achieve targeted gene delivery to hepatocytes, galactose has been shown to be a promising targeting ligand to hepatocytes (liver parenchymal cells) because these cells possess a large number of asialoglycoprotein receptors that recognize the galactose units on the glycoproteins or synthetic galactosylated carriers (Kawakami et al., 2002). Recently, we have developed several types of macromolecular and particulate gene carriers for hepatocyte-selective gene transfection in vivo (Kawakami et al., 2000; Fumoto et al., 2003a, 2004; Morimoto et al., 2003). These include galactosylated cationic liposomes containing Gal-C4-Chol, which can be efficiently recognized by asialoglycoprotein receptors in hepatocytes in vivo (Kawakami et al., 2000; Fumoto et al., 2004). However, a number of possible barriers are associated with in vivo gene delivery (Yang and Huang, 1997; Li et al., 1999; Sakurai et al., 2001a; Fumoto et al., 2003b). Detailed information regarding these barriers is needed to allow the rational design of effective gene carriers.

When galactosylated liposome/pDNA complex (lipoplex) was injected into the portal vein of mice, most of it was taken up by the liver (Kawakami et al., 2000). However, the level of in vivo gene expression was not as high as that expected from the in vitro results. Thus, there must be several barriers associated intrinsically with in vivo situations, such as convective blood flow in the liver, passage through the sinusoids,

This work was supported in part by grants-in-aid for Scientific Research from the Ministry of Education, Culture, Sports, Science, and Technology of Japan, by Health and Labor Sciences Research Grants for Research on Hepatitis and Bovine Spongiform Encephalopathy from the Ministry of Health, Labor and Welfare of Japan, by a grant-in-aid from the Mochida Memorial Foundation for Medical and Pharmaceutical Research, and by the 21st Century Center for Excellence Program "Knowledge Information Infrastructure for Genome Science."

Article, publication date, and citation information can be found at http://jpet.aspetjournals.org.

doi:10.1124/jpet.105.089516.

ABBREVIATIONS: Gal-C4-Chol, cholesten-5-yloxy-*N*-(4-((1-imino-2-D-thiogalactosylethyl)amino)butyl)formamide; pDNA, plasmid DNA; DOTMA, *N*-[1-(2,3-dioleyloxy)propyl]-*n*,*n*,*n*-trimethylammonium chloride; Chol, cholesterol; lipoplex, cationic liposome/pDNA complex; Rh-DOPE, 1,2-dioleoyl-*sn*-glycero-3-phosphoethanolamine-*N*-(lissamine rhodamine B sulfonyl); BSA, bovine serum albumin; Gal-BSA, galactosylated BSA; AUC, area under the curve; PC, parenchymal cells; NPC, nonparenchymal cells; IFN-γ, interferon-γ; MRT, mean residence time; FRET, fluorescent resonance energy transfer.

and tissue interactions. To elucidate these barrier processes, we investigated the hepatic disposition profiles of galactosylated lipoplex in rat liver perfusion experiments (Fumoto et al., 2003b), which allowed us to determine the uptake characteristics of a range of substances under different experimental conditions with the structure of the liver remaining intact. In our study, we demonstrated that the penetration of the galactosylated lipoplex through the hepatic fenestrated endothelium to the parenchymal cells was greatly restricted in perfused rat liver (Fumoto et al., 2003b).

It has been reported that lipoplex is able to interact with various types of biological components (e.g., serum proteins) because of their strong positive charge (Mclean et al., 1999; Sakurai et al., 2001b). The presence of serum proteins has been also thought to be a limiting factor for in vitro transfection by lipoplex. Understanding the interaction with the blood cells as well as serum proteins is crucial for the successful development of an effective gene delivery vector. However, the effects of interaction between the galactosylated lipoplex and blood components on asialoglycoprotein receptor-mediated gene transfer have not been well documented. Because the galactosylated lipoplex must pass through the endothelial cell barriers to reach the hepatocytes, the interaction between blood components and galactosylated lipoplex needs to be examined in detail.

In this study, we evaluated the effects of blood components (whole blood and serum) on physicochemical properties, the in situ and in vivo disposition, and the in vivo transfection efficiency of galactosylated lipoplex.

Materials and Methods

Materials. *N*-(4-Aminobutyl)carbamic acid *tert*-butyl ester and DOTMA were obtained from Tokyo Chemical Industry Co. Ltd. (Tokyo, Japan). Chol and Clear-Sol I were obtained from Nacalai Tesque (Kyoto, Japan), and Soluene 350 was purchased from PerkinElmer Life and Analytical Sciences (Boston, MA). Cholesteryl chloroformate and collagenase type IA were obtained from Sigma-Aldrich (St. Louis, MO). Rh-DOPE was purchased from Avanti Polar Lipids (Alabaster, AL). [α-^{32}P]dCTP (3000 Ci/mmol) was obtained from GE Healthcare (Little Chalfont, Buckinghamshire, UK). Galactosylated bovine serum albumin (Gal-BSA) as a ligand of asialoglycoprotein receptors was synthesized as described in our earlier study (Nishikawa et al., 1995). All other chemicals were of the highest purity available.

Animals. Female 5-week-old ICR mice (20–23 g) and male Wistar rats (170–210 g) were purchased from the Shizuoka Agricultural Cooperative Association for Laboratory Animals (Shizuoka, Japan). All animal experiments were carried out in accordance with the Principles of Laboratory Animal Care as adopted and promulgated by the National Institutes of Health (Bethesda, MD) and the Guidelines for Animal Experiments of Kyoto University.

Construction and Preparation of pDNA. pCMV-luciferase was constructed by subcloning the HindIII/XbaI firefly luciferase cDNA fragment from pGL3-control vector (Promega, Madison, WI) into the polylinker of pcDNA3 vector (Invitrogen, Carlsbad, CA). pDNA was amplified in the *Escherichia coli* strain DH5α, isolated, and purified using a QIAGEN Endofree Plasmid Giga Kit (QIAGEN GmbH, Hilden, Germany). Purity was confirmed by 1% agarose gel electrophoresis followed by ethidium bromide staining, and the pDNA concentration was measured by UV absorption at 260 nm. The pDNA for in vivo distribution and in situ liver perfusion experiments was labeled with [α-^{32}P]dCTP by nick translation (Sambrook et al., 1989).

Synthesis of Gal-C4-Chol. Gal-C4-Chol was synthesized as reported previously (Kawakami et al., 1998). In brief, cholesteryl chloroformate and *N*-(4-aminobutyl)carbamic acid *tert*-butyl ester were reacted in chloroform for 24 h at room temperature. A solution of trifluoroacetic acid and chloroform was added dropwise, and the mixture was stirred for 4 h at 4°C. The solvent was evaporated to obtain *N*-(4-aminobutyl)-(cholesten-5-yloxyl)formamide, which was then combined with 2-imino-2-methoxyethyl-1-thiogalactoside, and the mixture was stirred for 24 h at 37°C. After evaporation, the resultant material was suspended in water, dialyzed against distilled water for 48 h (12 kDa cut-off dialysis tubing), and then lyophilized.

Preparation of Galactosylated Cationic Liposomes. Mixtures of DOTMA, Chol, and Gal-C4-Chol were dissolved in chloroform at a molar ratio of 2:1:1 for galactosylated liposomes, vacuum-desiccated, and resuspended in sterile 5% dextrose solution at a concentration of 4 mg of total lipids/ml. The suspension was sonicated for 3 min, and the resulting liposomes were extruded 10 times through double-stacked 100-nm polycarbonate membrane filters.

Preparation of Galactosylated Lipoplex. Four hundred and twenty microliters of 286 μg/ml pDNA in 5% dextrose solution was mixed with an equal volume of galactosylated cationic liposomes at 1657 μg/ml and incubated for 30 min. The mixing ratio of liposomes and pDNA was expressed as a ($\pm$)-charge ratio, which is the molar ratio of cationic lipids to pDNA phosphate residues (Yang and Huang, 1997). A charge ratio of unity was obtained with 2.52 μg of total lipid/μg pDNA for galactosylated liposomes in this study. As far as the charge ratio was concerned, we selected a charge ratio of +2.3 for all experiments to obtain the most effective transfection activity for receptor-mediated gene transfer (Kawakami et al., 2000, 2004) and to prevent any effect of free liposomes (Eastman et al., 1997; Sakurai et al., 2001a). The particle size and ζ-potential of the galactosylated lipoplex were measured using a dynamic light-scattering spectrophotometer (LS-900; Otsuka Electronics, Osaka, Japan) and a laser electrophoresis ζ-potential analyzer (LEZA-500T; Otsuka Electronics), respectively.

Preparation of Serum and Whole Blood. Mouse or rat serum was prepared by the method of Sakurai et al. (2001a). In brief, mouse serum was isolated from fresh whole blood obtained from ICR mice. Blood was collected from the vena cava under anesthesia without heparin treatment and allowed to stand for 3 h at 37°C and then overnight at 4°C. Serum was collected after centrifugation. Inactivated serum was prepared by heating serum for 30 min at 56°C. Whole blood was collected in a heparinized syringe from ICR mice. An erythrocyte suspension was prepared as described in a previous report (Senior et al., 1991) by washing whole blood three times with phosphate-buffered saline (pH 7.4).

In Vivo Transfection Experiments. Before intraportal injection, galactosylated lipoplex was incubated with blood components for 5 min at 37°C. Mice were anesthetized by intraperitoneal administration of 50 mg/kg pentobarbital sodium. An incision was made in the abdomen, and the portal vein was exposed. The lipoplex preincubated with blood components was injected into the portal vein at a volume of 15 ml/kg, and the abdomen was closed with wound clips. Liver samples were taken 6 h after injection, and each sample was homogenized with lysis buffer (0.1 M Tris/HCl containing 0.05% Triton X-100 and 2 mM EDTA, pH 7.8). After three cycles of freezing and thawing, the homogenates were centrifuged at 10,000*g* for 10 min at 4°C. Twenty microliters of each supernatant was mixed with 100 μl of luciferase assay solution (Picagene; Toyo Ink Mfg. Co. Ltd., Tokyo, Japan), and the light produced was immediately measured using a luminometer (Lumat LB 9507; Berthold Technologies, Bad Wildbad, Germany). The protein content of the samples was determined using a protein quantification kit (Dojindo Molecular Technologies Inc., Gaithersburg, MD). For evaluation of the intrahepatic localization of gene expression, the luciferase activities in the liver parenchymal (PC) and nonparenchymal cells (NPC) were independently determined after centrifugal separation of PC and NPC in

collagenase-digested liver as previously described (Kawakami et al., 2000). In the inhibition experiments involving hepatic transfection, mice received intravenous injections of 20 mg/kg Gal-BSA 1 min before the intraportal injection of the lipoplex.

In Vivo Distribution Study. ^{32}P-Labeled galactosylated lipoplex preincubated with blood components was injected into the portal vein of mice at a volume of 15 ml/kg. At each collection time point, blood was collected from the vena cava and mice were killed at the end of the experiment. The liver, kidneys, spleen, heart, and lungs were removed, washed with saline, blotted dry, and weighed. Ten microliters blood and a small amount of each tissue were digested with 0.7 ml of Soluene-350 by incubating overnight at 45°C. After digestion, 0.2 ml of isopropanol, 0.2 ml of 30% hydroperoxide, 0.1 ml of 5 M HCl, and 5.0 ml of Clear-Sol I were added. The samples were stored overnight, and the radioactivity was measured in a scintillation counter (LSA-500; Beckman Coulter, Inc., Fullerton, CA).

Calculation of Organ Uptake Clearance. Tissue distribution data were evaluated using organ uptake clearances as reported previously (Takakura et al., 1987). In brief, the tissue uptake rate can be described by the following equation,

$$\frac{dX_t}{dt} = \mathrm{CL_{uptake}} \times \mathrm{C_b} \quad (1)$$

where X_t is the amount of ^{32}P-labeled galactosylated lipoplex in the tissue at time t, $\mathrm{CL_{uptake}}$ is the tissue uptake clearance, and C_b is the blood concentration of ^{32}P-labeled galactosylated lipoplex. Integration of eq. 1 gives the following,

$$X_t = \mathrm{CL_{uptake}} \times \mathrm{AUC_{(0-t)}} \quad (2)$$

where area under the curve $(\mathrm{AUC})_{(0-t)}$ represents the area under the blood concentration time curve from time 0 to t. The $\mathrm{CL_{uptake}}$ value can be obtained from the initial slope of a plot of X_t versus $\mathrm{AUC_{(0-t)}}$.

Liver Perfusion Experiments and Pharmacokinetic Analysis. In situ liver perfusion studies were carried out as reported previously (Nishida et al., 1989; Fumoto et al., 2003b). In brief, the portal vein was catheterized with a polyether nylon catheter (SURFLO i.v. catheter, 16 G'2"; Terumo Co., Tokyo, Japan) and immediately perfused with Krebs-Ringer-bicarbonate buffer supplemented with 10 mM glucose (oxygenated with 95% O_2 and 5% CO_2, adjusted to pH 7.4 at 37°C). The perfusate did not contain serum proteins and blood cells. The perfusate was circulated using a peristaltic pump (SJ-1211; Atto Bioscience, Tokyo, Japan) at a flow rate of 13 ml/min. After a stabilization period of 25 min, ^{32}P-labeled galactosylated lipoplex preincubated with rat serum or whole blood (30 μg of pDNA/300 μl) was administered via the portal vein using a six-position rotary valve injector (Type 50 Teflon rotary valves; Rheodyne Inc., Cotati, CA). After the addition of 5 ml of Clear-Sol I, the radioactivity of the effluent perfusate was measured in a scintillation counter (LSA-500, Beckman Coulter, Inc., CA). The outflow patterns were analyzed by statistical moment analysis. In brief, the AUC and mean residence time (MRT) were calculated as follows:

$$\mathrm{AUC} = \int_0^\infty C dt \quad (3)$$

$$\mathrm{MRT} = \int_0^\infty tCdt/\mathrm{AUC} \quad (4)$$

where t is the time and C is the concentration of ^{32}P-labeled galactosylated lipoplex. The moments can be calculated by numerical integration using a linear trapezoidal formula and extrapolation to infinite time based on a monoexponential equation (Yamaoka et al., 1978). The t values were corrected for the lag time of the catheter. The recovery ratio (F) and extraction ratio (E) were derived from F = AUC · Q (flow rate) and $E = 1 - F$, respectively.

The outflow patterns were also analyzed based on a two-compartment dispersion model, where sinusoidal and binding compartments were considered. The mass balance equations involving the axial dispersion in the sinusoidal space are as follows:

$$\frac{\partial C_S(t,z)}{\partial t} + v\frac{\partial C_S(t,z)}{\partial z} = D\frac{\partial^2 C_S(t,z)}{\partial z^2} - k_{12} \times C_S(t,z) + \varepsilon k_{21} \times C_B(t,z) \quad (5)$$

$$\frac{\partial C_B(t,z)}{\partial t} = \frac{1}{\varepsilon} k_{12} \times C_S(t,z) - k_{21} \times C_B(t,z) - k_{int} \times C_B(t,z) \quad (6)$$

where $C_S(t, z)$ and $C_B(t, z)$ are the concentrations of drug in the sinusoidal space and binding compartment, respectively, D is the dispersion coefficient, ϵ is the volume ratio of the binding compartment to the sinusoidal space in the liver, k_{12} and k_{21} are the forward and backward partition rate constants between the sinusoidal space and binding compartment, k_{int} is the first-order internalization rate constant from the binding compartment to the intracellular space, v is the linear flow velocity of the perfusate, t is time, and z is the axial coordinate in the liver. The initial and boundary conditions are given as follows:

$$C_S(t, 0) = M/Q \times f_I(t),\ C_S(0, z) = 0,\ C_S(t, \infty) = 0,\ C_B(t, 0) = 0,\ C_B(0, z) = 0 \quad (7)$$

where M is the amount of drug injected into the liver, Q is the flow rate of the perfusate, and $f_I(t)$ has the dimension of the reciprocal of time. Taking the Laplace transform with respect to t, rearranging, substituting the length of the sinusoidal space L with z, and introducing the cross-sectional area of the sinusoidal space A, the following image equation is obtained as follows:

$$\tilde{C}_S(s) = \frac{M}{Q}\tilde{f}_I(s);\ \exp\left[\left\{\frac{Q}{2D_C} - \sqrt{\left(\frac{Q}{2D_C}\right)^2 + \frac{1}{D_C}\left\{s + k_{12} - \frac{k_{12} \times k_{21}}{s + k_{21} + k_{int}}\right\}}\right\}V_S\right] \quad (8)$$

where $\tilde{C}_S(s)$ and $\tilde{f}_I(s)$ denote the Laplace transform of the concentration in the venous outflow and input function $f_I(t)$, respectively, D_C is the corrected dispersion coefficient ($D_C = D \cdot A^2$), V_S is the sinusoidal volume (= L · A), and the flow rate Q is equal to A × v.

Each parameter (D_C, k_{12}, k_{21}, k_{int}, and V_S) was calculated by curve-fitting of the Laplace-transformed equation to the experimental venous outflow pattern using a nonlinear least-squares program with a fast inverse Laplace transform algorithm MULTI (FILT) (Yano et al., 1989). The damping Gauss-Newton method with no constraint was used for curve-fitting with the MULTI algorithm. Herein, $f_I(t)$ was assumed to be a Δ function, because the lipoplexes were rapidly injected using a six-rotary valve injector.

For evaluation of the intrahepatic localization of the amounts taken up, 30 min after injection of ^{32}P-labeled galactosylated lipoplex into the isolated perfused liver, the radioactivities in the liver PC and NPC were separately determined after centrifugal separation of PC and NPC in collagenase-digested liver as described previously (Fumoto et al., 2003b).

Observation of Dissociation of pDNA and Lipids from Lipoplex Induced by Mixing with Blood. Carboxy-fluorescein labeling of pDNA was performed using the Label IT Fluorescein Nucleic Acid Labeling Kit (Mirus Co., Madison, WI). Liposomes were labeled with Rh-DOPE at 2% (mol/mol) total lipid. Fluorescent-labeled lipoplex was then prepared by mixing fluorescein-labeled pDNA with rhodamine-labeled liposomes as described above. To observe the dissociation of pDNA and lipids from lipoplex induced by whole blood, fluorescent-labeled lipoplex was mixed with 30% blood and subsequently centrifuged and the erythrocytes were washed twice with phosphate-buffered saline. To investigate the effect of

TABLE 1
Effect of preincubation with serum on the particle size and ζ potential of galactosylated lipoplex
Results are expressed as the mean ± S.D. of three experiments. Statistical comparisons were performed using an unpaired Student's t test.

Incubation	Mean Particle Size	ζ Potential
	nm	*mV*
None (control)	142.1 ± 7.20	35.8 ± 5.67
With serum	217.5 ± 1.08*	−16.2 ± 3.20*

* $P < 0.01$.

preincubation with serum, fluorescent-labeled lipoplex was mixed with 15% serum for 5 min and then mixed with 15% erythrocyte suspension to adjust the hematocrit. Lipoplex integrity was assessed by fluorescent resonance energy transfer (FRET) from fluorescein-pDNA to rhodamine lipids. Precipitates (i.e., lipoplex bound to blood cells) were mounted on glass slides, covered by slips, and observed by confocal laser-scanning microscope (MRC 1024; Bio-Rad, Hercules, CA). On the other hand, galactosylated lipoplex in the supernatant was measured by spectrofluorophotometry (RF540; Shimadzu Co., Kyoto, Japan). The excitation wavelengths were 480 and 550 nm for fluorescein pDNA and Rh-DOPE.

Agarose Gel Electrophoresis. The pDNA stability of the galactosylated lipoplex in blood was determined by agarose gel electrophoresis (Harvie et al., 2000). The galactosylated lipoplex was preincubated with blood components at 37°C. After incubation, pDNA was extracted from the mixture by phase separation using phenol/chloroform/isoamyl alcohol (25:24:1) followed by precipitation with ethanol. Precipitated pDNA was redissolved with Tris borate-EDTA buffer, pH 8.0, and subjected to agarose gel electrophoresis. Densitometric analysis was performed using a commercially available computer program [CS analyzer; Atto Bioscience and Rise Corporation, Sendai, Japan].

Serum IFN-γ Concentration Measurement. Blood was collected 6 h after intraportal injection of galactosylated lipoplex, simultaneously with the in vivo transfection experiment, and was subsequently allowed to stand for 3 h at 4°C. Serum was collected after centrifugation and frozen at −80°C until measurement. The serum IFN-γ concentration was determined using commercially available enzyme-linked immunosorbent assay kits (OptEIA mouse IFN-γ set; BD Biosciences, San Jose, CA).

Statistical Analysis. Statistical comparisons were performed by an unpaired Student's t test for two groups or Dunnett's test for multiple comparisons with a control group. Statistical comparisons in the transfection experiments and serum IFN-γ measurements were performed by the Mann-Whitney test for two groups or Steel's test for multiple comparisons with a control group because of the heterogeneity of the variance evaluated by the F test and Bartlett test, respectively.

Results

Effect of Blood Components on the Physicochemical Characteristics of Galactosylated Lipoplex. To investigate the effect of serum protein on the physicochemical characteristics of galactosylated lipoplex, the particle size and ζ-potential were measured after exposure to mouse serum because these parameters affect the hepatic disposition of galactosylated lipoplex (Fumoto et al., 2003b). Mixing with serum [30% (v/v)] significantly enlarged the particle size of the lipoplex (Table 1). The ζ-potential of the galactosylated lipoplex was significantly reduced by mixing with serum, and the charge became negative, suggesting that negatively charged serum proteins covered much of the galactosylated lipoplex surface. These results are consistent with our previous report about the conventional lipoplex (Sakurai et al., 2001a).

After mixing galactosylated lipoplex with erythrocyte suspension, hemagglutination was observed. However, mixing galactosylated lipoplex with whole blood did not induce any obvious hemagglutination (data not shown), suggesting that the presence of serum components prevents hemagglutination. Recently, Eliyahu et al. (2002) also reported similar results with the conventional lipoplex. Thus, galactosylated lipoplex was mixed with whole blood to evaluate the effect of blood cells on transfection activity.

Transfection Activities of Galactosylated Lipoplex Preincubated with Blood Components. To study the effect of blood components on in vivo transfection activity, galactosylated lipoplex was preincubated with serum or whole blood before administration and the transfection activities in the liver were evaluated 6 h after intraportal injection to mice. When the galactosylated lipoplex was preincubated with serum, the hepatic transfection activities were enhanced approximately 20- to 70-fold (Fig. 1A). However, incubation with whole blood [30% (v/v)] reduced the transfection activity in the liver by 97% (Fig. 1B). These results show that the interaction with blood cells markedly inhibits the hepatic transfection activity of galactosylated lipoplex. In addition, higher concentration of blood components exhibited

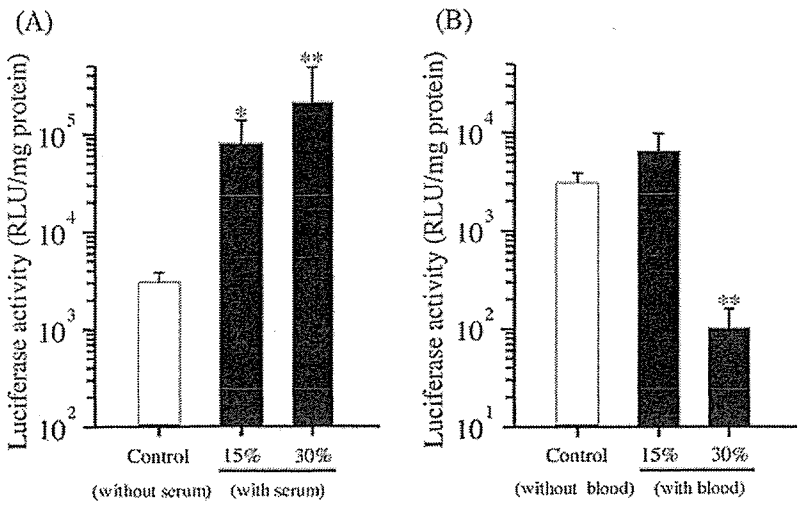

Fig. 1. Effect of preincubation with serum (A) or whole blood (B) on the hepatic transfection activity of galactosylated lipoplex after intraportal injection in mice. pDNA (30 μg) was complexed with galactosylated liposomes at a charge ratio of +2.3. Five minutes before injection, the lipoplexes were mixed with serum or whole blood at the indicated volume ratio. Luciferase activity was determined 6 h postinjection of the lipoplex. Each value represents the mean ± S.D. of at least three experiments. Statistical comparisons with the control group were performed by Steel's test (*, $P < 0.05$; **, $P < 0.01$). RLU, relative light unit.

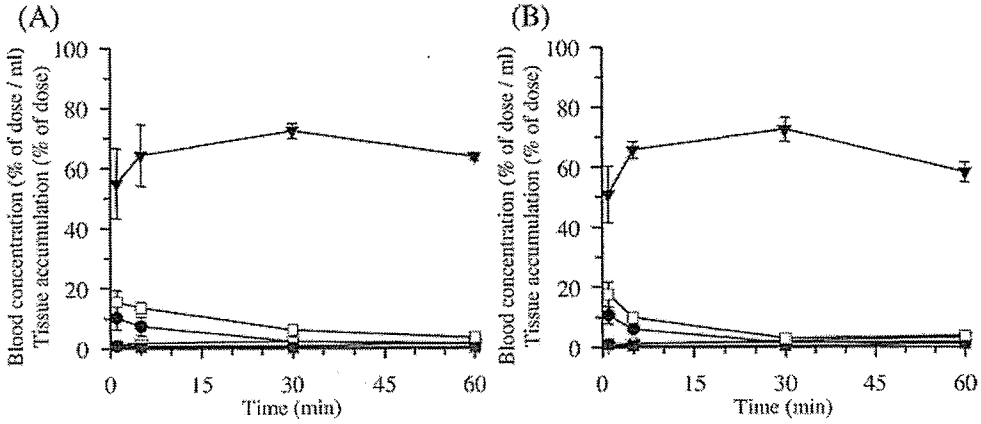

Fig. 2. Effect of preincubation with serum on the distribution of galactosylated lipoplex after intraportal injection in mice. [^{32}P]pDNA (30 μg) was complexed with galactosylated liposomes at a charge ratio of +2.3. Five minutes before injection, galactosylated lipoplex was mixed without (A) or with (B) 30% serum. Radioactivities were determined in the blood (●), lung (□), liver (▼), kidney (○), spleen (▽), and heart (■). Each value represents the mean value ± S.D. of at least three experiments.

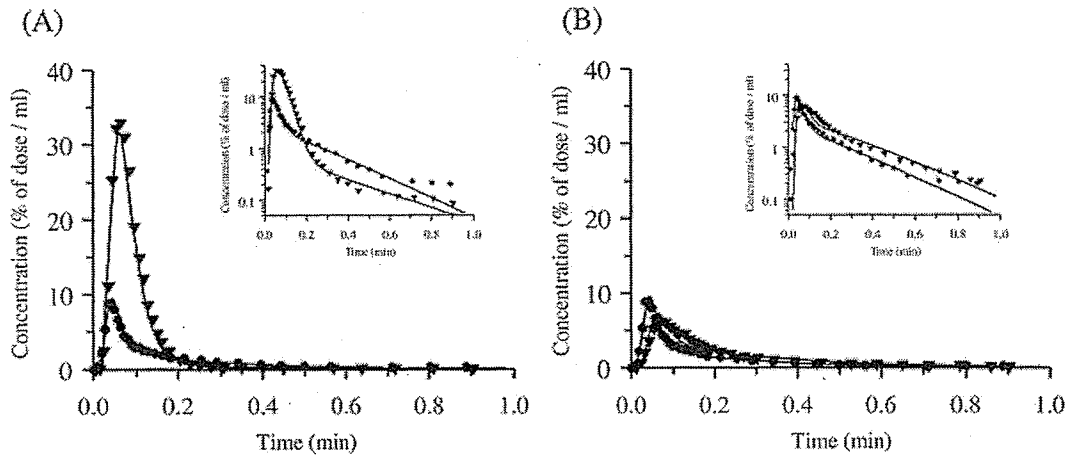

Fig. 3. Typical venous outflow patterns of ^{32}P-labeled galactosylated lipoplex with 30% serum (A) and with 30% whole blood (B) in perfused rat liver. The insets show semilogarithmic plots. The curves simulated by a two-compartment dispersion model are also shown in these figures. Circle symbols represent control, and inverted triangles represent incubation with serum (A) or whole blood (B).

more marked effect on transfection activity. In in vivo condition, blood volume is larger than the volume of the lipoplex solution. Thus, the result of 30% blood or serum would be more close to in vivo condition than the result of 15% blood components. Therefore, we applied 30% blood components as the experimental condition for further studies.

In Vivo Distribution of Galactosylated Lipoplex Preincubated with Serum. To investigate why the transfection activity of galactosylated lipoplex was enhanced by incubation with serum, the biodistribution of galactosylated lipoplex preincubated with serum was evaluated using ^{32}P-labeled galactosylated lipoplex (Fig. 2). However, similar distribution patterns

TABLE 2

Effect of incubation with serum or whole blood on the moment parameters for galactosylated lipoplex in the liver perfusion experiments

Results are expressed as the mean ± S.D. of three experiments. Statistical comparisons with the no incubation group were performed by Dunnett's test.

Incubation	AUC	MRT	E
	% of dose · s/ml	*s*	*%*
None (control)	62.0 ± 5.05	14.9 ± 1.03	87.0 ± 1.04
With serum	177 ± 13.9*	7.96 ± 0.56*	65.3 ± 1.94*
With whole blood	79.4 ± 2.43	18.6 ± 2.95	83.2 ± 1.22**

* $P < 0.01$; ** $P < 0.05$.

TABLE 3

Effect of incubation with serum or whole blood on the model parameters for galactosylated lipoplex in the liver perfusion experiments

Results are expressed as the mean ± S.D. of three experiments. Statistical comparisons with the no incubation group were performed by Dunnett's test.

Incubation	k_{12}	k_{21}	k_{12}/k_{21}	k_{int}
	min^{-1}			*min^{-1}*
None (control)	33.9 ± 4.33	1.68 ± 0.35	20.4 ± 2.31	3.88 ± 0.43
With serum	14.5 ± 1.12*	0.27 ± 0.04*	53.8 ± 2.98*	3.02 ± 0.06**
With whole blood	28.8 ± 2.39	3.63 ± 0.30*	8.00 ± 1.36*	4.22 ± 0.35

* $P < 0.01$; ** $P < 0.05$.